UNIVERSITATEA BABEȘ-BOLYAI
Facultatea de Chimie și Inginerie Chimică

SYNTHESIS, STRUCTURE AND SUPRAMOLECULAR PROPERTIES OF NEW CRYPTANDS AND THE ACCESS TOWARDS MECHANICALLY INTERLOCKED MOLECULES

PhD Student
Cosmin V. CRIȘAN

Scientific advisor
Prof. Dr. Ion GROSU

Cluj-Napoca
September 2020

UNIVERSITATEA BABEȘ-BOLYAI

Facultatea de Chimie și Inginerie Chimică

Jury:

President:

Acad. Prof. Dr. Cristian Silvestru	Babeș-Bolyai University

Reviewers:

Prof. Dr. Csaba Paizs	Babeș-Bolyai University
Conf. Dr. Habil. Ileana C. Fărcășanu	University of Bucharest
Conf. Dr. Anamaria E. Terec	Babeș-Bolyai University
CS I Dr. Claudiu Filip	INCDTIM Cluj-Napoca

Cluj-Napoca

September 2020

Table of Contents

Chapter 1. INTRODUCTION....1

1.1. Macrocyclic molecules....1

1.2. Macrocycles and molecular recognition....1

1.3. Binding forces in molecular recognition....2

1.4. Mechanically interlocked molecules....3

1.4.1. Rotaxanes....4

1.4.2. Catenanes....4

1.4.3. Synthetic strategies for MIM's....5

Chapter 2. OBJECTIVES....13

Chapter 3. RESULTS AND DISSCUSSIONS....15

3.1. Synthesis of cage molecules displaying a non-symmetrical cavity....15

3.1.1. Towards non-symmetrical cryptands with 2,4,6-triphenyl-1,3,5-triazine and/or 1,3,5-triphenylbenzene aromatic units and m-xylene/pyridyl bridges....15

3.1.2. Synthesis of non-symmetrical cryptands with 2,4,6-triphenyl-1,3,5-triazine aromatic units and oligoethyleneoxide/pyridyl bridges....22

3.2. Synthesis of cage molecules displaying symmetrical cavity....35

3.2.1. Cryptands with 2,4,6-triphenyl-1,3,5-triazine and/or 1,3,5-triphenylbenzene aromatic units and oligoethyleneoxide bridges....36

3.2.2. Towards more rigid cryptands with 1,3,5-triazine aromatic units to act both as anchor groups and bridges....46

3.2.3. Cryptands with 2,4,6-triphenyl-1,3,5-triazine or 1,3,5-triphenylbenzene aromatic units and pyridyl bridges....49

Chapter 4. APPLICATIONS....67

4.1. Investigations on cryptand's 33 properties towards new mechanically interlocked cryptand-macrocycle assemblies....67

4.2. Investigations on cryptand's 33 properties towards new crypto-catenanes....73

4.3 Complexation properties of cryptands 21, 22 and 23....88

Chapter 5. CONCLUSIONS....98

Chapter 6. EXPERIMENTAL PART....100

6.1. General remarks....100

6.2. Experimental procedures....101

Chapter 1. INTRODUCTION

In the fascinating world of chemistry beyond molecule, macrocyclic structures have always been at the core of the most important discoveries, demonstrating their versatility in a wide range of research areas. The accelerating technological progress that we witness nowadays is rooted, amongst others, in the development of new materials that made possible the creation of machines and devices with progressively smaller size. Out of the full array of molecules that are exploited in the research applied to nanoscience, cryptands, in particular, proved to be an important asset, due to their peculiar design that allows for a wide range of applications, starting from optoelectronics and ending with molecular machines, the study of which, brings us closer to understanding the intricate mechanisms that govern the natural world. The research presented in this thesis explores two significant areas in which the cryptands play an important part: molecular recognition and mechanically interlocked architectures, which, in many cases, lay the foundation of molecular machines.

Chapter 2. OBJECTIVES

The present work is framed on the synthesis of new macrocyclic structures and the study regarding the properties and applicability of the newly attained compounds. Therefore, two main objectives are outlined:

The first objective is the synthesis of new cyclophanes and cage molecules, displaying either symmetrical or non-symmetrical cavity as well as possessing different sized apertures of the binding sites. The symmetrical target molecules are based on extended C_3 symmetric scaffolds, while the non-symmetrical ones are constructed through the use of a modular approach. The extended scaffolds are designed to provide a larger cavity which is suitable for encapsulating more complex molecules. Furthermore, an increased aperture can provide more space for intertwining other ring-shaped molecules around the arms of the cryptand or even within the cavity. **Figure 2** depicts the simplified schematic representation of the target compounds.

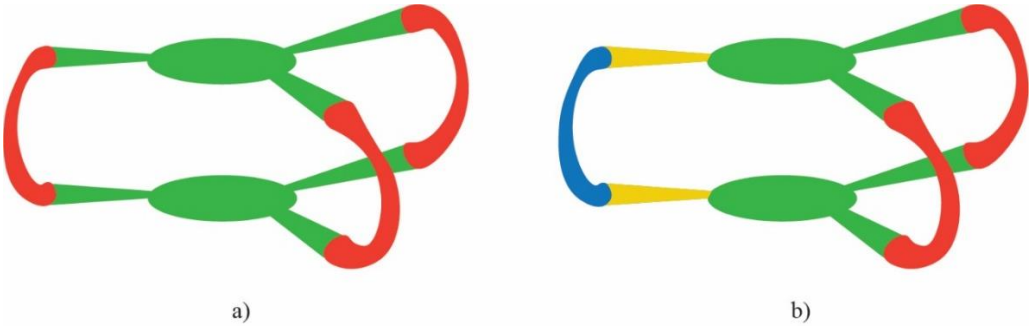

Figure 1. *Schematic representation of the target molecules.*

Several different strategies were envisioned as a means of attaining the cage molecules with both symmetrical and unsymmetrical bridges. Thereby, in the case of the cryptands with symmetrical cavities (**Figure 1a**), two synthetic approaches were investigated: i) *via* direct (one step) macrocyclization and ii) by applying a two-step strategy based on the preparation of a tripodand first, followed by a subsequent macrocyclization reaction. Regarding the cage molecules with unsymmetrical cavities (**Figure 1b**), a multi-step strategy was envisioned, starting from a de-symmetrized scaffold which is employed in the synthesis of a macrocycle with two identical bridging units. After attaching a suitable functional group on each of the macrocycle's scaffolds, a second macrocyclization reaction is conducted, which results in the formation of the unsymmetrical cage molecule.

The second objective involves the study of the properties and applicability in molecular recognition of the newly obtained structures, as well investigating the potential of certain cryptands in accessing higher order architectures, such as cryptand-macrocycle interlocked assemblies, through the employment of the active metal template synthetic strategy.

Chapter 3. RESULTS AND DISSCUSSIONS

3.1.1. Towards non-symmetrical cryptands with 2,4,6-triphenyl-1,3,5-triazine and/or 1,3,5-triphenylbenzene aromatic units and *m*-xylene/pyridyl bridges

Considering the potential and the overall research interest for non-symmetrical cage compounds, we envisioned a modular approach for achieving this type of architectures, which provides a more accurate control over the cage functionalization by allowing the introduction of

specific functional groups in subsequent stages of the synthetic process (**Scheme 1**). A key component in the development of the target molecules is the non-symmetric "central units" which enables further functionalization and thus allowing the introduction of different bridges. Our synthetic approach was based on the non-symmetrical substituted 1,3,5-triazine and phenylene moieties **III** which, by the means of a macrocyclization reaction with two identical bridges leads to the formation of a [2+2]-cyclophane **II**. The macrocycle is then functionalized so as to allow a second macrocyclization reaction with a different type of bridging molecule and thus to grant the formation of a non-symmetrical [2+2+1] type cryptand **I**.

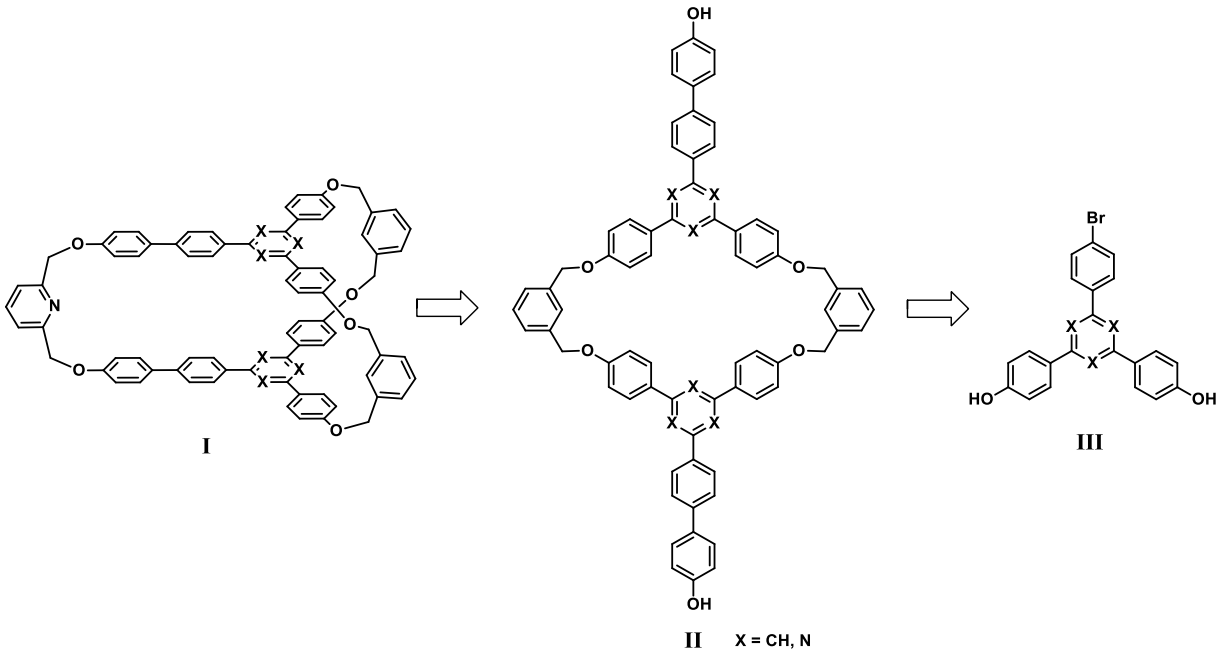

Scheme 1. *Retrosynthetic scheme for the synthesis of type **I** cryptands.*

The initial step of the synthetic approach consisted in the synthesis of the non-symmetrical 1,3,5-triazine unit which was performed by adapting a cyclotrimerization procedure that has been previously used in our research group[1] for obtaining the triazine triphenol **5** (**Scheme 2**). Instead of reacting only 4-hydroxybenzonitrile alone and thus obtaining the triphenol, we decided to introduce 4-bromobenzonitrile alongside 4-hydroxybenzonitrile in the cyclotrimerization process. The reaction yielded a mixture of three differently substituted 1,3,5-triazines, as shown in **Scheme 2**.

[1] A. Woiczechowski-Pop, I. L. Dobra, G. D. Roiban, A. Terec, I. Grosu, *Synth. Commun*. **2012**, *42*, 3579.

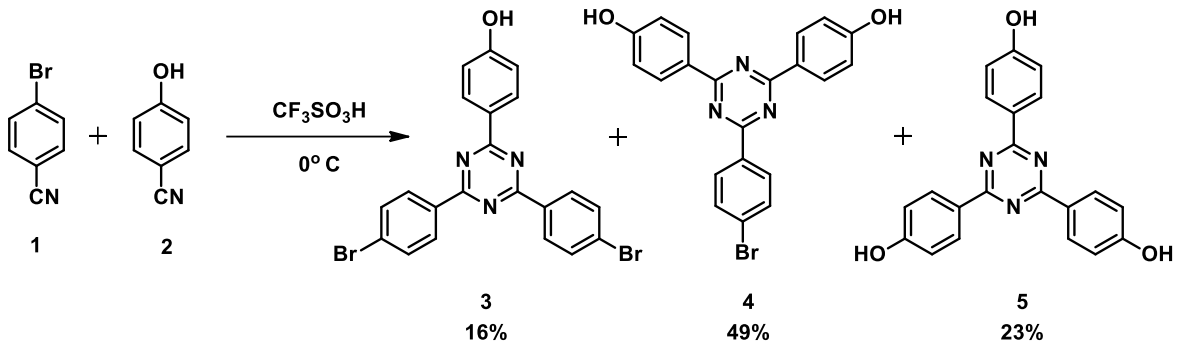

Scheme 2. *Synthesis of 1,3,5-triazine derivatives **3-5**.*

After isolating each compound, triazine **4** was employed in the next step of the synthetic strategy, while triphenol **5** was exploited for the synthesis of cryptands with symmetrical cavities, a subject matter that will be presented in detail in the next chapter. Therefore, we proceeded to the synthesis of cyclophane **6** by reacting compound **4** with the commercially available *m*-xylylene dibromide (**Scheme 3**).

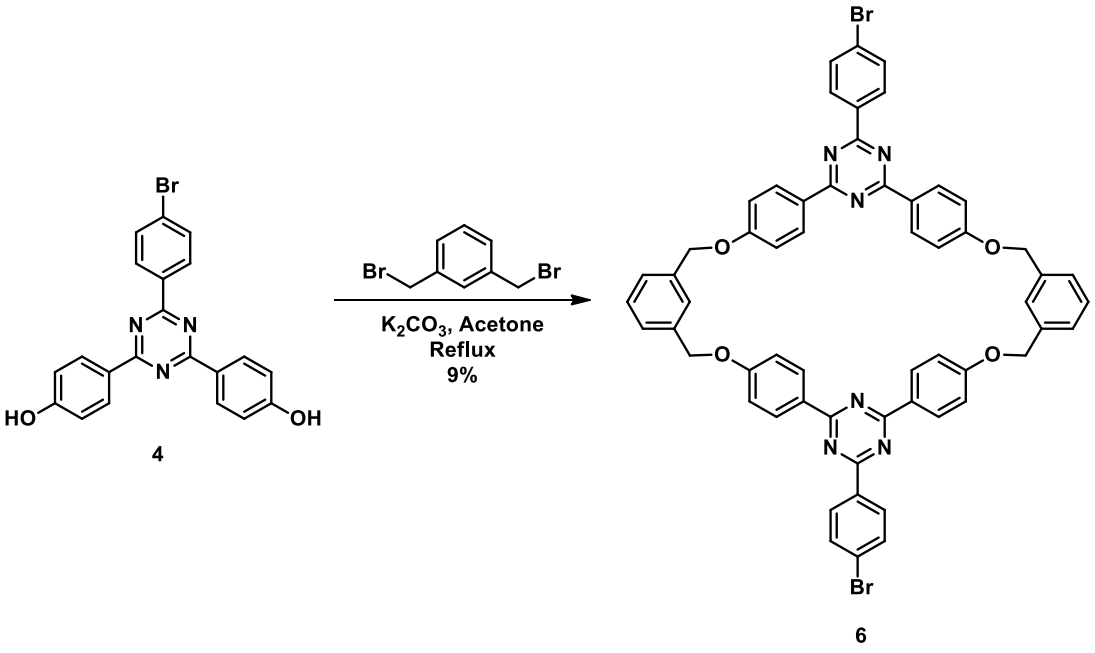

Scheme 3. *Synthesis of macrocycle **6**.*

The macrocyclization reaction was performed in acetone at refluxing temperature over the course of 72 hours affording compound **6** with a modest 9% yield. Despite numerous efforts directed at improving the yield by changing various parameters of the reaction, no significant

increases were observed. After purification, the derivative **6** was characterized using mass spectrometry and NMR spectroscopy before proceeding to the next key step of the synthetic strategy which consisted in the functionalization of the cyclophane so as to accommodate a third bridge and thus bringing us one step closer to the formation of the desired non-symmetrical cryptand. Therefore, compound **6** was decorated with an additional *p*-hydroxybenzene moiety at each end, having the double-purpose of both functionalizing the macrocycle for the next stage and increasing the cavity size of the resulting cryptand (**Scheme 4**).

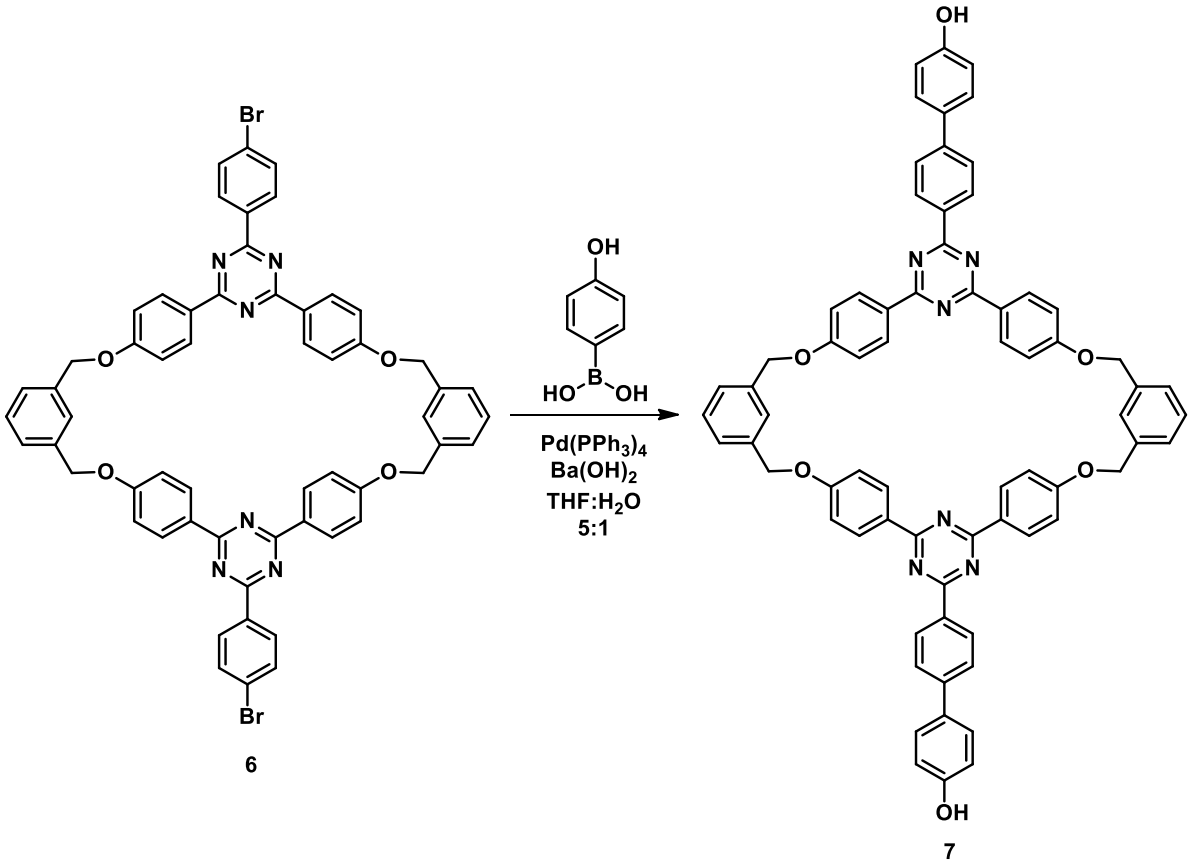

Scheme 4. *Decoration of macrocycle **6** with p-hydroxybenzene units via Suzuki coupling conditions.*

The functionalization of macrocycle **6** was performed *via* a Suzuki cross-coupling reaction with the commercially available 4-hydroxyphenylboronic acid. The reaction occurred at refluxing temperature in a mixture of THF and water (5:1), having $Ba(OH)_2$ as base and tetrakis(triphenylphosphine)palladium(0) as catalyst. Although an ESI(+)-MS experiment performed on the crude of the reaction indicated that the formation of the target compound **7** might

be possible, the structure of the macrocycle could not be confirmed by other characterization methods, even after several purification attempts.

Simultaneously, we investigated a second approach, this time employing the non-symmetrically functionalized triphenyl-benzene unit **11** (**Scheme 5**) *in lieu* of the 1,3,5-triazine **4**, albeit following the same synthetic strategy. The triphenyl-benzene **11** was synthesized using an aldol condensation method previously reported in literature[2], by reacting 4'-hydroxyacetophenone with 4'-bromoacetophenone in presence of $SiCl_4$. After derivative **11** was isolated and characterized, the second step of the synthetic strategy was undertaken by employing the freshly obtained compound **11** with *m*-xylylene dibromide in a macrocyclization reaction using the same conditions as described for compound **6** (**Scheme 5**).

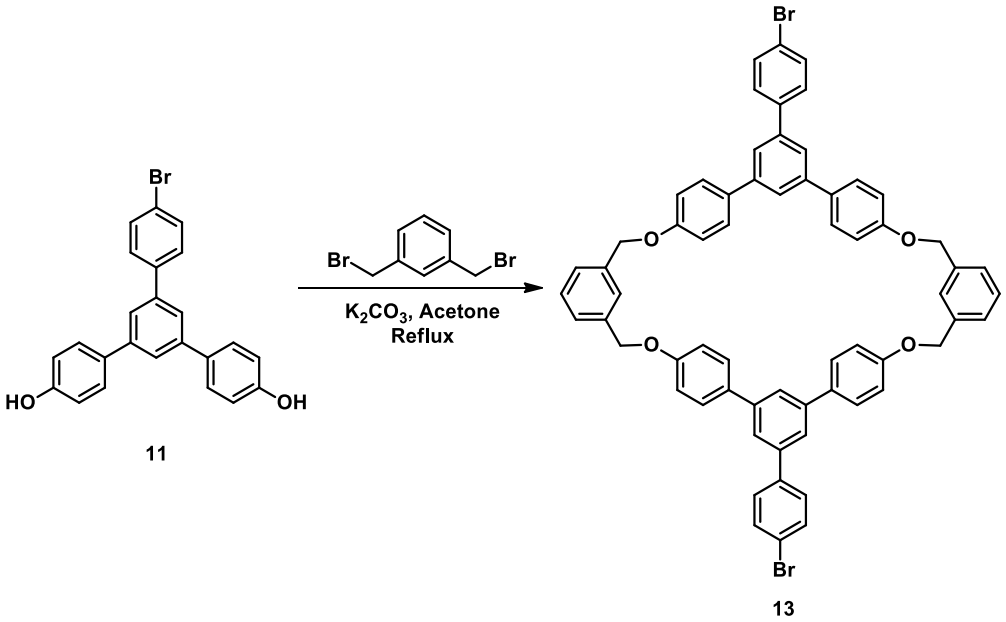

Scheme 5. *Synthesis of compound **13**.*

Both NMR spectroscopy and MS spectrometry confirmed the formation of the target compound **13**. However, although several purification attempts were made, the purity level attained was not acceptable for employing compound **13** in a subsequent reaction.

[2] M. Yang, S. Shi, M. Wang, Z. Luo, W. Qiu, Y. Wang, Z. Feng, T. Zhao, *Polym. Adv. Technol.* **2011**, *22*, 1471.

3.1.2. Synthesis of non-symmetrical cryptands with 2,4,6-triphenyl-1,3,5-triazine aromatic units and oligoethyleneoxide/pyridyl bridges

Having encountered numerous difficulties in the purification and solubility of the target macrocycles **6** and **13**, we decided to change the *m*-xylylene bridges with oligoethylene glycol tether chains as shown in **Scheme 6**. Furthermore, the chains would provide additional flexibility of the cage molecule and thus resulting in a more adaptative cavity that could bind more complex guest molecules. On a second note, we also investigated the versatility of this modular approach in obtaining different cryptands by simply varying the functional groups that decorates the type **V** macrocycle.

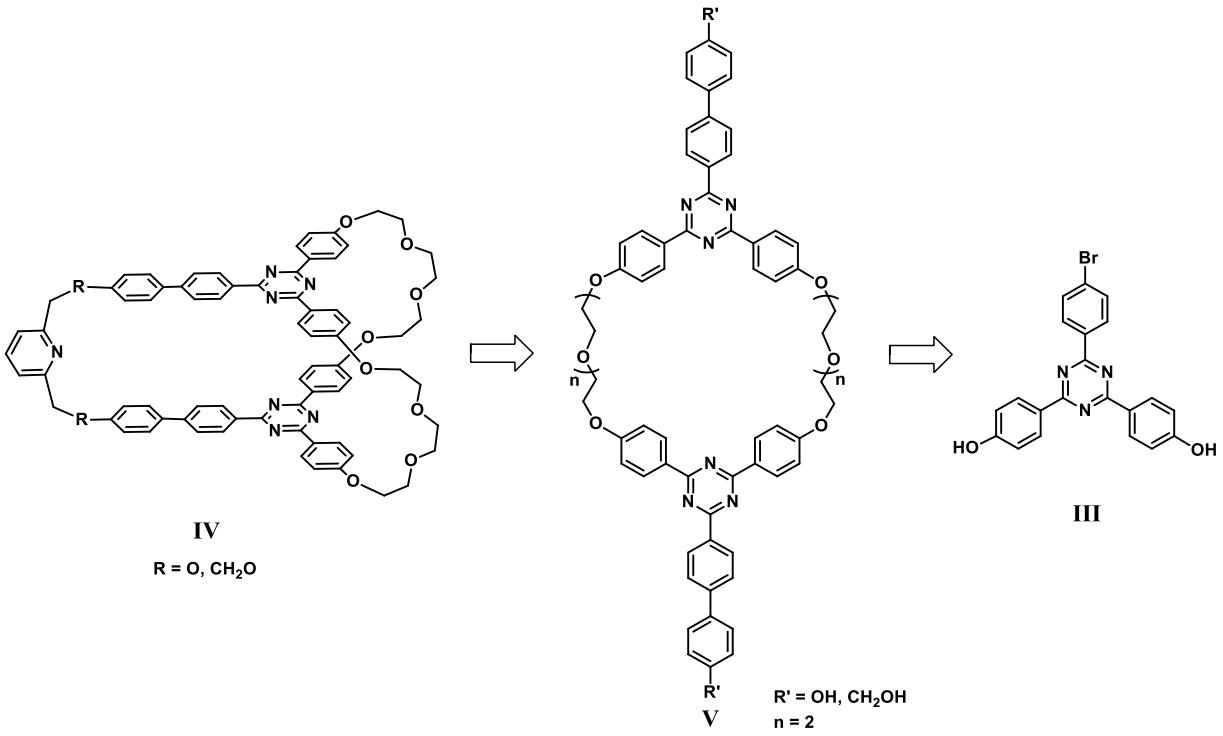

Scheme 6. *Retrosynthetic scheme for the synthesis of type **IV** molecular cages.*

The key element of this second route consisted in the use of same non-symmetrically substituted 1,3,5-triazine unit **4**, employed in the first synthetic strategy, but deciding to ditch the triphenyl-benzene unit due to poor performance in attempts of synthesizing both symmetrical and non-symmetrical cage molecules. Therefore, starting from the triazine derivative **4**, we decided to investigate a series of four macrocycles (**Scheme 7**) in order to decide the simplest and most facile

route to the final target cryptand. Consequently, macrocycles **14**, **15** and **16** were obtained as a result of a direct macrocyclization between derivative **4** and the corresponding ditosylated oligoethylene glycols.

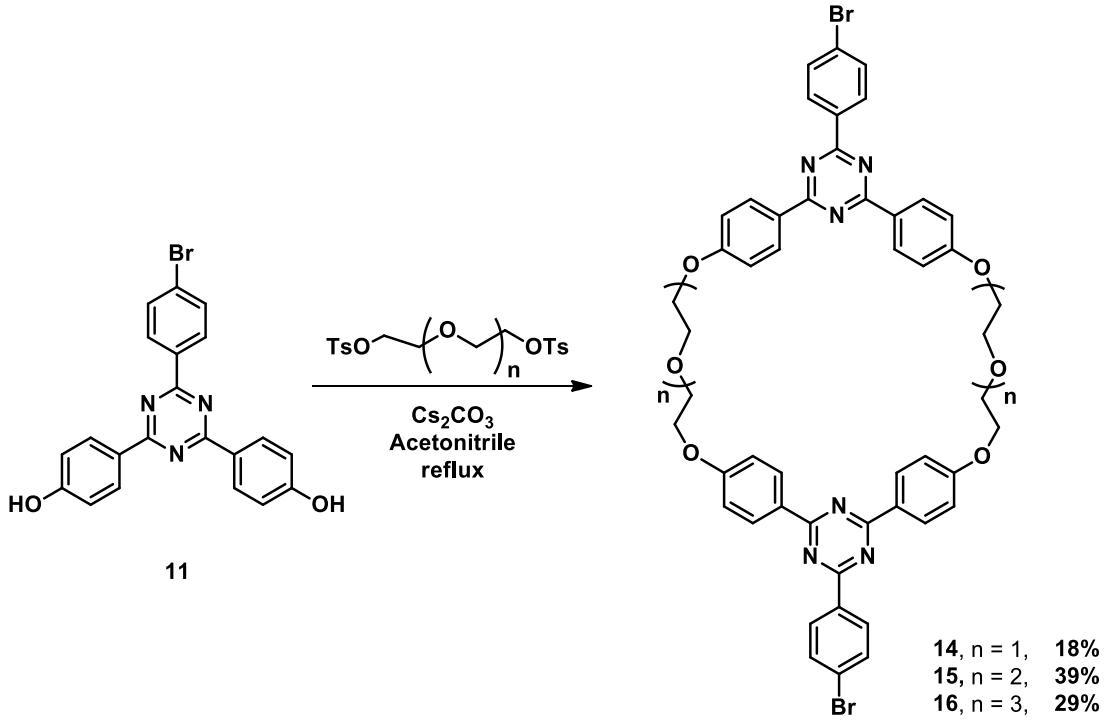

Scheme 7. *Preparation of macrocycles **14**–**16** using oligoethyleneglycol tether chains.*

The outcome of the reaction afforded the desired macrocycles with yields ranging from 18% to 39%, depending on the oligoethyleneglycol used, as shown in **Scheme 7**. Therefore, the highest yielding result was given by the employment of the ditosylated triethylene glycol as bridging unit. Also worth mentioning is the fact that the macrocycle attained by using ethylene glycol as tether chain was characterized by mass spectrometry and NMR spectroscopy, but due to the low purity and small quantity obtained, the yield of the reaction was not calculated.

Having achieved, over several attempts, the highest yield from the series of the four macrocycles, compound **15** was selected for the next stage in the synthetic strategy, which consisted in decorating the macrocycle with a suitable functional unit that facilitates the construction of the target cryptands *via* a subsequent macrocyclization reaction (**Scheme 8**).

Similar to the previously discussed compound **6** we investigated the functionalization of the macrocycle with two phenol units that were added by means of a Suzuki cross-coupling reaction

(**Scheme 8**). The conditions chosen were again tetrakis(triphenylphosphine)palladium(0) as catalyst and $Ba(OH)_2$ as base, the reaction being performed in a mixture of THF and water (4:1).

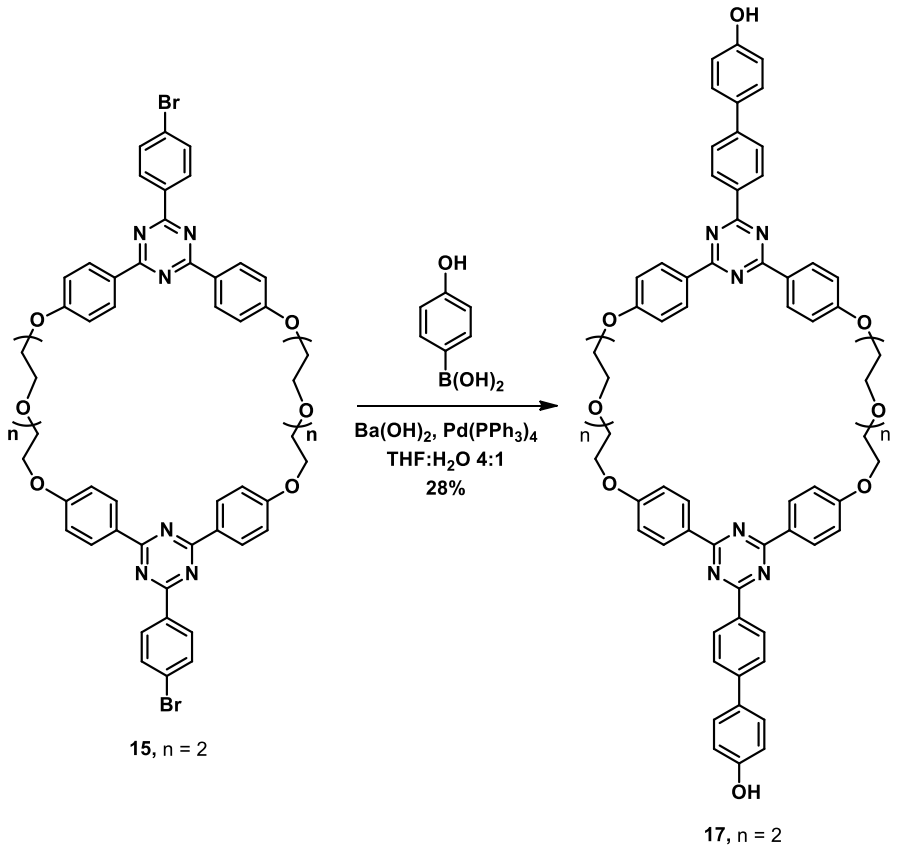

Scheme 8. *Preparation of macrocycle **17** using Suzuki cross-coupling conditions.*

After purification, the reaction afforded compound **17** with a 28% yield and the isolated compound was characterized by NMR spectroscopy and mass spectrometry before moving on to the next stage.

The final step of the synthetic approach consisted in adding a third bridge to compound **17** and thus 'locking' the macrocycle in a permanent cage-like structure as shown in **Scheme 9**.

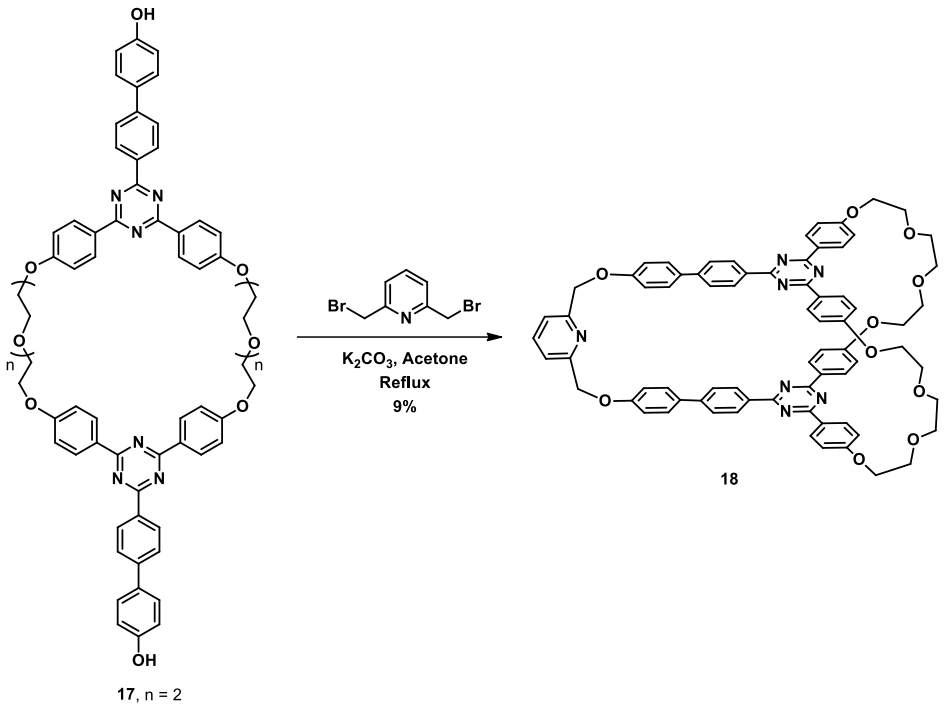

Scheme 9. *Synthesis of the non-symmetric cage molecule **18**.*

The bridge chosen to carry out this task was 2,6-bis(bromomethyl)pyridine which performed well as a building block in the synthesis of both symmetric and non-symmetric cage molecules. Furthermore, the pyridine was chosen for its ability to participate in the coordination of various metal ions which proves to be a convenient asset for developing higher order supramolecular architectures[3]. Therefore, the macrocyclization reaction between compound **17** and 2,6-bis(bromomethyl)pyridine was carried out in high dilution conditions over the course of 48 hours, affording the desired derivative **18** with a 9% yield. After purification, the structure of the isolated product was validated by NMR spectroscopy and mass spectrometry.

Concurrently, we designed a second cryptand similar to compound **17**, but with an additional methylene group, which, after inserting a third bridge in the subsequent step of the strategy, would lead to the formation of the target cage molecule (see **Scheme 6**). The additional methylene group would increase the bridge flexibility leading to a more adaptative cavity and thus encouraging the encapsulation of a wider spectrum of guest molecules. Moreover, the introduction of the methylene group, places the oxygen atoms in a more favorable position, allowing them to participate in the coordination of metal ions to the pyridyl bridge and thus stabilizing the whole

[3] J. D. Crowley, S. M. Goldup, A.-L. Lee, D. A. Leigh, R. T. McBurney, *Chem. Soc. Rev.* **2009**, *38*, 1530.

complex. This stabilization facilitates the intertwining of other macrocyclic molecules around the pyridyl bridge and thus allowing the development of more complex mechanically interlocked architectures. In this regard, the modular strategy adopted proved once again its flexibility, being able to convert the end product by simply changing the functional group employed when decorating the macrocycle **15**. Therefore, the introduction of an additional methylene was made possible by changing the 4-hydroxyphenylboronic with 4-hydroxymethylbenzeneboronic acid, as shown in **Scheme 10**.

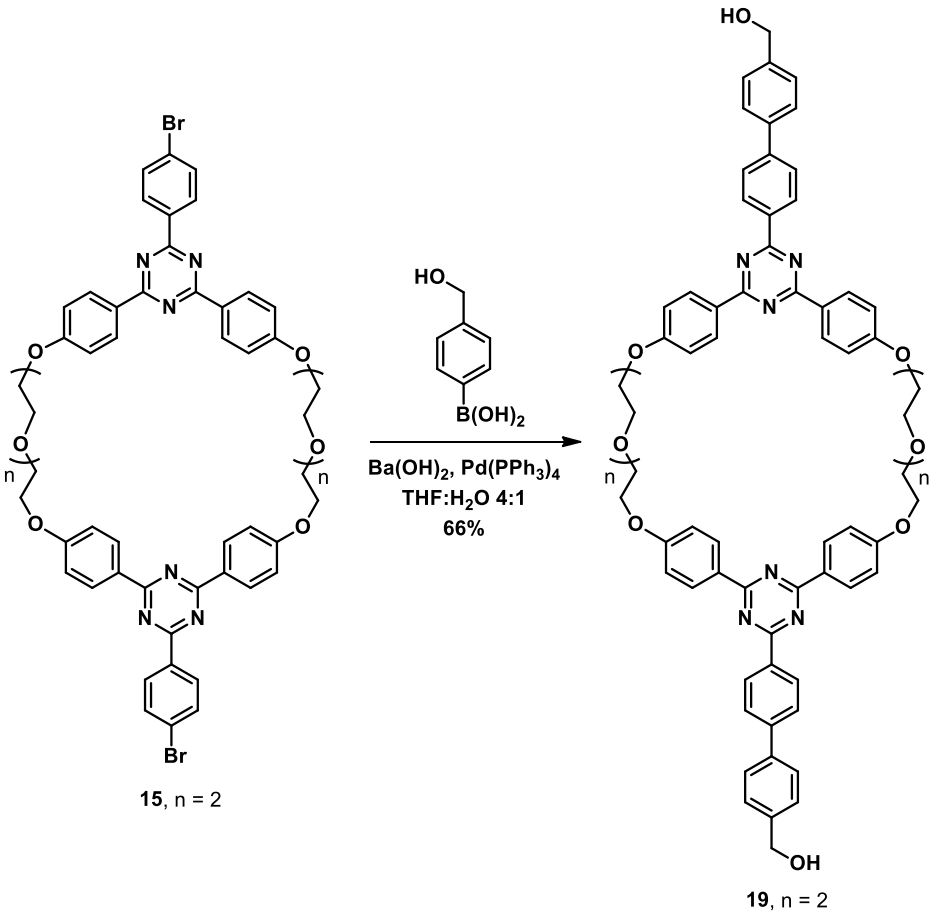

Scheme 10. *Preparation of derivative **19** via Suzuki cross-coupling conditions using 4-hydroxymethylbenzeneboronic acid.*

The reaction occurred in identical conditions as for compound **17**, but the yield was significantly improved to 66% instead of the 28% for the case of macrocycle **17**. The analytical methods employed in the structural characterization of the isolated compound **19** were NMR spectroscopy (^{1}H, ^{13}C) along with mass spectrometry. The ES(+)-MS spectrum displayed the

molecular peak while also revealing the affinity of compound **19** for alkali metal ions such as Na^+ and K^+, respectively.

Having successfully completed the last step before the final macrocyclization reaction, we proceeded to the synthesis of the target cryptand **20** by reacting macrocycle **19** with 2,6-bis(bromomethyl)pyridine and thus inserting the final bridge to the [2+2+1] cryptand (**Scheme 11**).

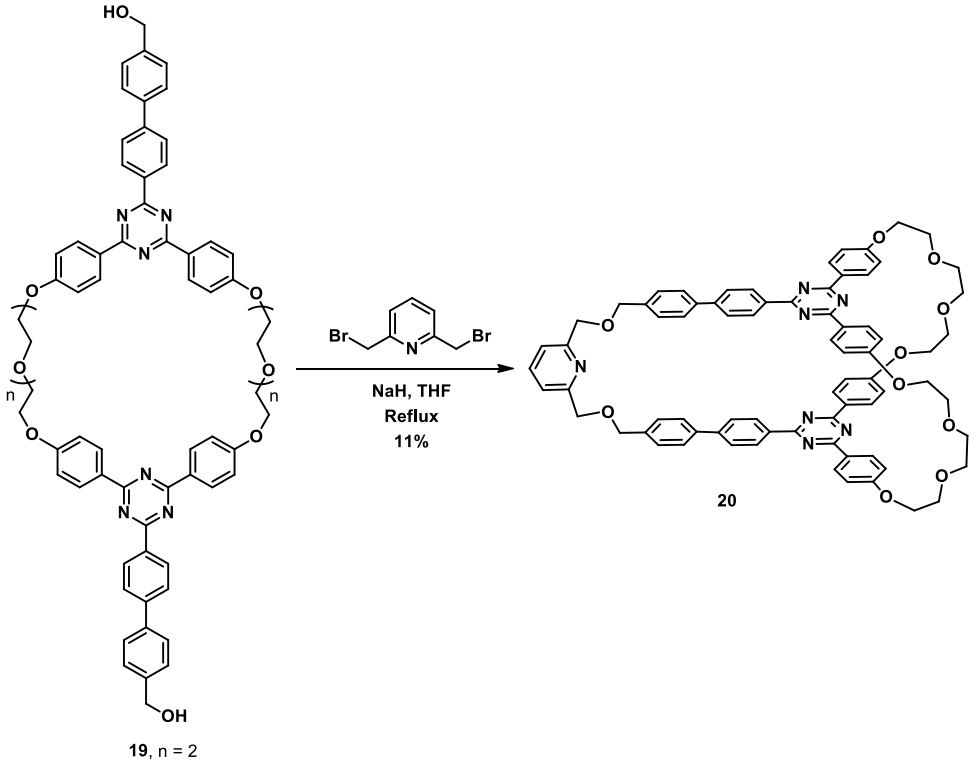

Scheme 11. *Preparation of cryptand **20**.*

The macrocyclization reaction was performed in anhydrous THF using NaH as base. After purification on column chromatography, the target compound **20** was isolated with a 11% yield and its structure characterized by NMR and MS studies.

3.2.1. Cryptands with 2,4,6-triphenyl-1,3,5-triazine and/or 1,3,5-triphenylbenzene aromatic units and oligoethyleneoxide bridges

Considering the importance of the triazine scaffold, we found it of great interest to synthesize cryptands with 2,4,6-triaryl-1,3,5-triazine core units (**Chart 1**), exhibiting tether chains

of various lengths (by altering the number of ethyleneoxide units employed). The variable lengths of the bridging units generate a more flexible cavity, which might allow the encapsulation of one or more guests, as observed in similar cases.[4] Furthermore, we decided to investigate the structure of these new host molecules and their ability to complex aromatic guests (e.g., 1,5-diaminonaphthalene) or alkali metal cations.

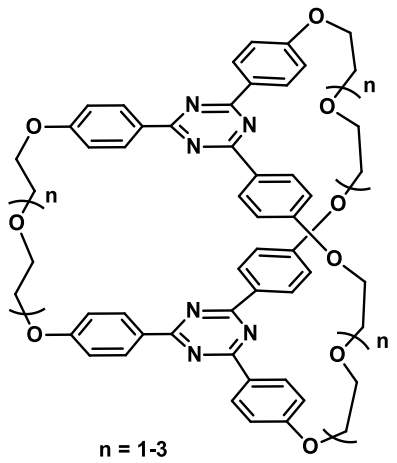

Chart 1. *General representation of the target cryptands with triazine units and oligoethyleneoxide bridges.*

In order to access the target cryptands, two synthetic strategies were investigated, as shown in (**Scheme 12**).

[4] (a) A. Das, S. Ghosh, *Angew. Chem., Int. Ed.* **2014**, *53*, 2038; (b) Y.Kikuchi, K. Ono, K. Johmoto, H.Uekusa, N. Iwasawa, *Chem. Eur. J.* **2014**, *20*, 15737; (c) T. Han, C.-F. Chen, *Org. Lett.* **2007**, *9*, 4207; (d) G. H. Clever,W. Kawamura, S. Tashiro, M. Shiro, M. Shionoya, *Angew. Chem., Int. Ed.* **2012**, *51*, 2606; (e) T. Murase, K. Otsuka, M. Fujita, *J. Am. Chem. Soc.* **2010**, *132*, 7864.

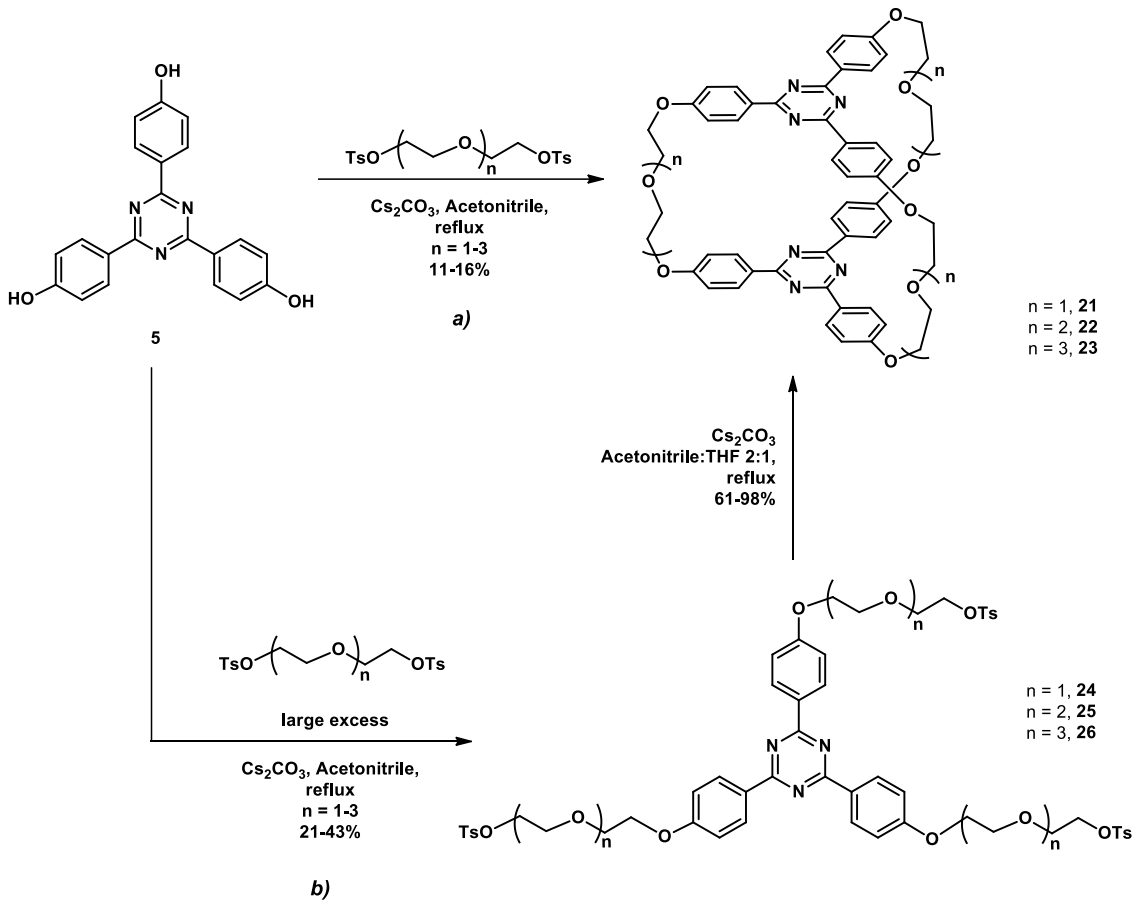

Scheme 12. *Synthesis of cryptands **21**-**23**.*

The first route (**Scheme 12a**) consisted in a one-step synthetic approach, involving a direct macrocyclization of the triazine triphenol **5** with the selected ditosylated oligoethylene glycols. The reactions took place in acetonitrile, under high dilution conditions, in presence of Cs_2CO_3 as base and template. After purification on column chromatography, the desired cryptands were isolated in moderate yields ranging from 11% to 16% and their structure was characterized by NMR spectroscopy and mass spectrometry.

The second synthetic strategy (**Scheme 12b**) was designed to optimize the access route to the desired cryptands by further increasing the overall yields. The approach consisted in a two steps strategy based on the preparation of tripodands **24**-**26** as intermediates, followed by a subsequent macrocyclization reaction with the triazine derivative **5**. The tripodands were synthesized by reacting triphenol **5** with a stoichiometric excess of the corresponding ditosylated oligoethylene glycols. After purification on column chromatography, the structure of all synthesized compounds **24**-**26** was confirmed using NMR spectroscopy and MS spectrometry.

After purification, the isolated tripodands were reacted with the triazine derivative **5**, in high dilution conditions, in order to achieve the target cryptands. The overall yields were much better on the second strategic approach, compounds **21** and **22** being isolated with an average output of around 40%, the isolation and purification of the final products being considerably more facile in this case.

While having the upper hand in the overall yield, the two-step procedure also has the advantage of allowing the preparation of non-symmetrical cryptands that exhibit different aromatic groups. As a result, by following this procedure it is possible to synthesize cryptands with non-symmetrical cavities by changing the aromatic reagent from the macrocyclization reaction. To prove this concept, we decided to change the triazine derivative **5** with a triphenol exhibiting an 1,3,5-triphenylbenzene unit **12** and react it with the tripodand **24**, as shown in **Scheme 13**.

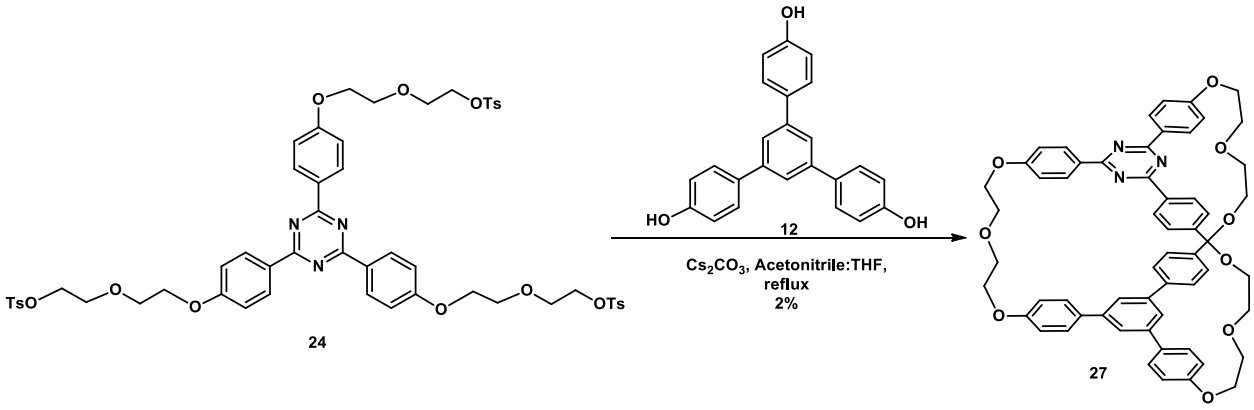

Scheme 13. *Synthesis of cryptand **27**.*

The reaction performed in conditions required for a macrocyclization led to non-symmetrical cryptand **27** showing both 2,4,6-triphenyl-1,3,5-triazine and 1,3,5-triphenylbenzene units. The synthesis of non-symmetrical cryptand **27** gave inferior yields (2% for the macrocyclization reaction with subsequent purification) and the separation of the pure compound by chromatography was considerably more difficult than in the cases of cryptands **21**-**23**.

Having successfully synthesized the series of cryptands by either direct macrocyclization or by following a two-step approach, we decided to investigate the consequences of employing a similar, but radically different central unit in the construction of the cryptands. Having the most facile purification and affording the best overall yield, compound **24** was chosen for comparison.

Therefore, we decided to compare the results, following the replacement of the 1,3,5-triazine unit in compound **24** with 1,3,5-triphenylbenzene, applying the synthetic strategy that proved to be the most efficient, namely the two-step approach.

The first step consisted in the synthesis of the podand, starting from the previously synthesized triphenol **12** and attaching the oxydiethylene chains, in the same manner as for podand **24** (**Scheme 14**).

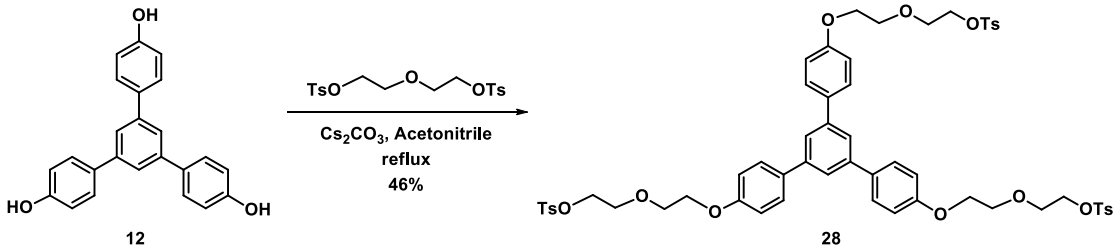

Scheme 14. *Synthesis of tripodand **28**.*

The reaction afforded the desired compound with a comparable yield (46% for **28** *vs.*43% for the previously synthesized podand **24**).

Having successfully obtained and characterized the podand **28**, the next step was undertaken by reacting it with triphenol **12** as shown in **Scheme 15**. The macrocyclization reaction was performed in identical conditions with those employed for synthesizing cryptand **27**, using MeCN as solvent and Cs_2CO_3 as base.

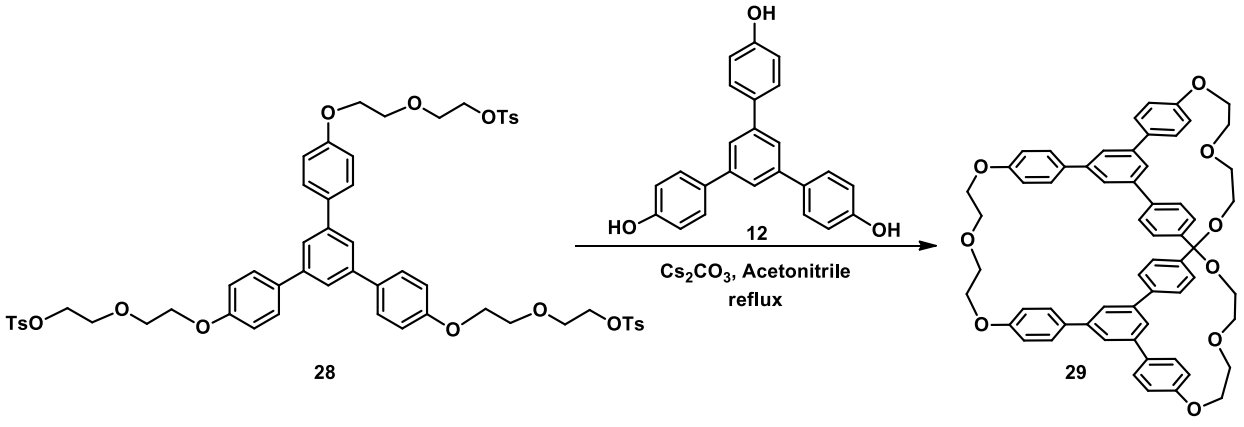

Scheme 15. *Synthesis of cryptand **29**.*

An APCI(+)-MS experiment performed on the crude of the reaction revealed the likely formation of the target derivative by displaying the molecular peak at *m/z* = 919.38. However, a multitude of other undesired by-products were present in both the MS spectrum and the TLC plate used for monitoring the reaction.

3.2.3. Cryptands with 2,4,6-triphenyl-1,3,5-triazine or 1,3,5-triphenylbenzene aromatic units and pyridyl bridges

Another type of cage molecules displaying symmetrical cavity was designed by introducing the pyridine moiety as the foundation for the cryptand's bridging units, as shown in **Chart 2**. The pyridine scaffold represents a key component in building host molecules due to its ability to form complexes with various aromatic compounds such as anthracene and pyrene[5] as well as with different metal ions such as copper (I) and palladium (II). The chelation of metal ions is an important asset that makes the pyridine a valuable building block in designing more complex supramolecular architectures such as catenanes, rotaxanes and knots.[6]

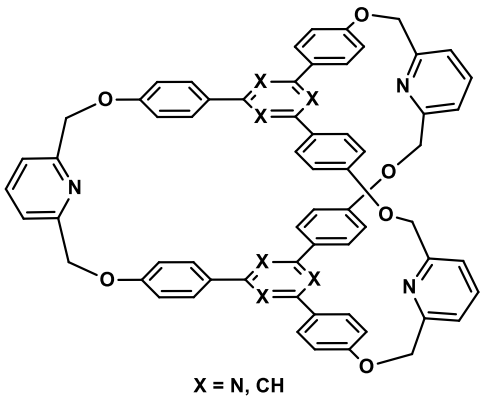

Chart 2. *General representation of the target cryptands with 2,4,6-triphenyl-1,3,5-triazine and/or 1,3,5-triphenylbenzene aromatic units and pyridyl bridges.*

An additional factor that influenced the design of the target cryptands is the cavity size, upon which the selectivity of a macrocyclic compound depends on.[7] Based on this premise, the

[5]C. Lar, A. Woiczechowski-Pop, A. Bende, I. G. Grosu, N. Miklasova, E. Bogdan, N. D. Hadade, A. Terec, I Grosu, *Beilstein J. Org. Chem.* **2018**, *14*, 1370.
[6] J. E. Beves, B. A. Blight, C. J. Campbell, D. A. Leigh, R. T. McBurney, *Angew. Chem. Int. Ed.* **2011**, *50*, 9260.
[7]C-S.Zuo, J-M.Quan, Y-D.Wu, *Org. Lett.* **2007**, *9*, 4219.

target molecules were designed to accommodate large aromatic components in their structure, with the purpose of improving aperture and thus increasing the size of the potential guest molecules that could be encapsulated. Furthermore, the design implied the use of oxygen atoms as bridging points between the components. The bridging oxygen can display various bond lengths and angles which determine the macrocycle to adopt diverse conformational structures with self-tuned cavity sizes as a response to the guest molecule.

Based on the aforementioned facts, we envisioned the synthesis of cryptand **33** (**Scheme 16**) starting from the commercially available 2,6-bis(bromomethyl)pyridine and the triazine triphenol **5**, both of which are employed in a macrocyclization reaction having acetone as solvent and K_2CO_3 as base.

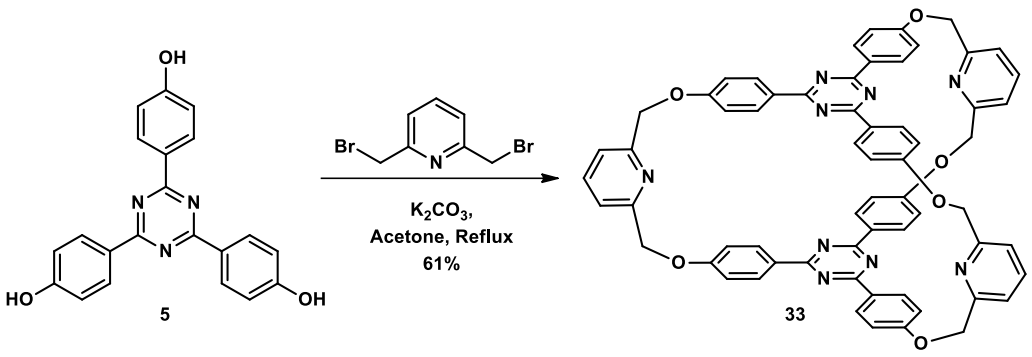

Scheme 16. *Synthesis of cryptand **33** bearing pyridyl bridges.*

The straight-forward design of the cryptand, combined with a facile purification, provided compound **33** with a surprisingly good yield (61%). The structure of the target cryptand **33** was confirmed by mass spectrometry and NMR spectroscopy, as well as X-ray diffraction studies.

The ES(+)-MS spectrum performed on the isolated product at room temperature displays the characteristic peak for the protonated species alongside a supplementary molecular peak which indicates the affinity of cryptand **33** towards copper ions due to the pyridine moieties that make up the bridging units.

Single crystals of **33** were obtained at room temperature by vapor diffusion between a 1,2-dichloroethane solution of **33** and ethanol. The X-ray diffraction revealed that the asymmetric unit consists of one molecule (**Figure 2**). The two 1,3,5-triazine units are almost on top, slightly rotated and parallel to each other with an angle between the planes defined by these rings of 4.5(1)°, an

average dihedral angle C–C_g–C_g'–C or N–C_g–C_g'–N of 36.3(1)° and a C_g–C_g' distance of 3.35 Å which suggests a π···π interactions (where C_g and C_g' are the centroids of the two triazine rings) (**Figure 3a**). Due to the rotation and orientation of the *p*-phenylene units relative to the 1,3,5-triazine rings, a propeller like arrangement can be identified within the molecule, with the unit cell containing two molecules, one with left- and the other one with a right-handed propeller arrangement (**Figure 3b**). The left/right-handed propeller arrangement is however consistent only for the C1–N1–C2–N2–C3–N3 triazine unit but not for the C23–N4–C24–N5–C25–N6 unit.

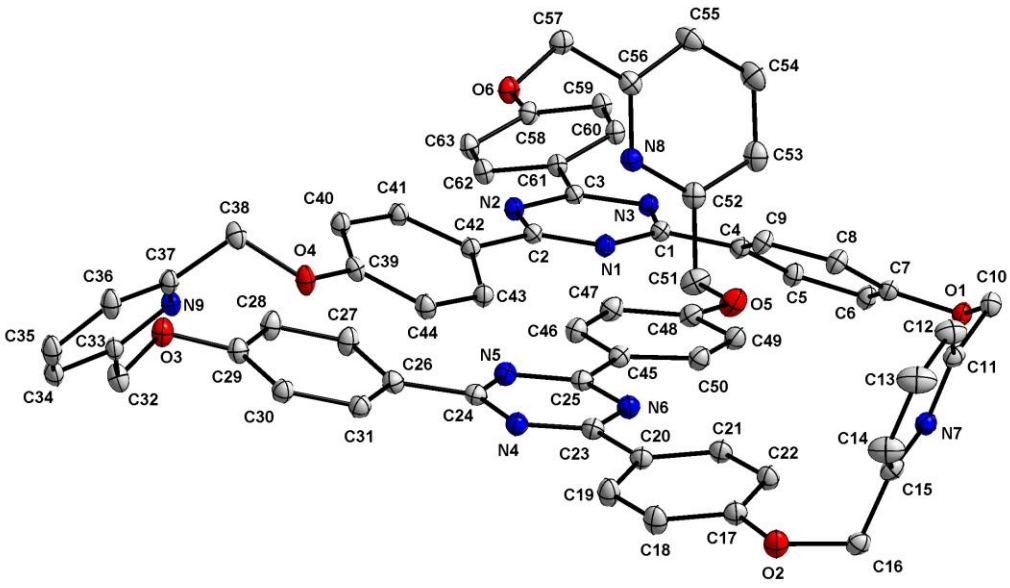

Figure 2. *View of the asymmetric unit in the crystal of **33**, shown with 40% probability ellipsoids (hydrogen atoms are omitted for clarity).*

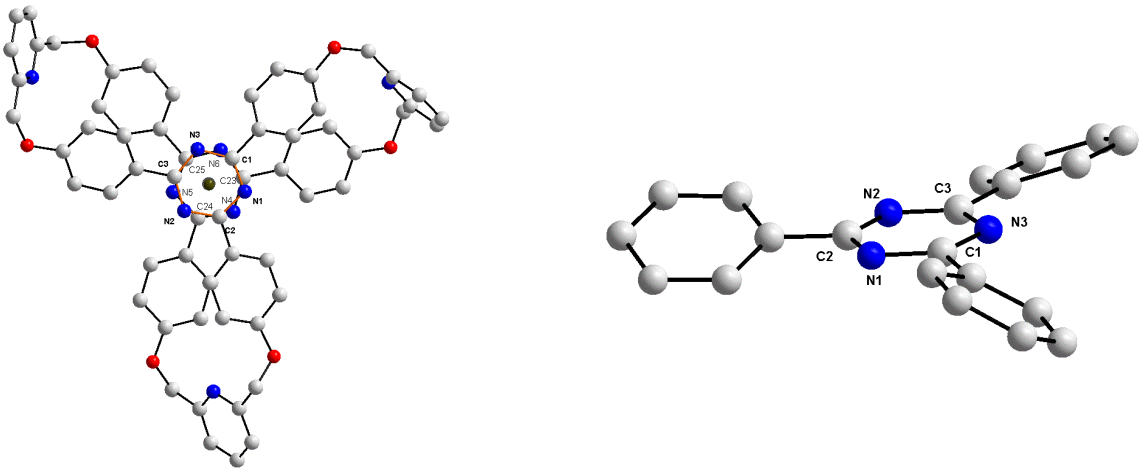

(a) (b)

Figure 3. *a) View of the asymmetric unit in the crystal of **33** showing the arrangement of the 1,3,5-triazine units; b) Fragment showing the propeller like arrangement of the p-phenylene rings attached to one of the 1,3,5-triazine units.*

Having successfully synthesized and characterized cryptand **33**, we envisioned a similar cryptand displaying the same pyridyl bridges (**Scheme 17**), but with 1,3,5-triphenylbenzene units instead of the 2,4,6-triaryl-1,3,5-triazine units that have been used for the construction of **33**.

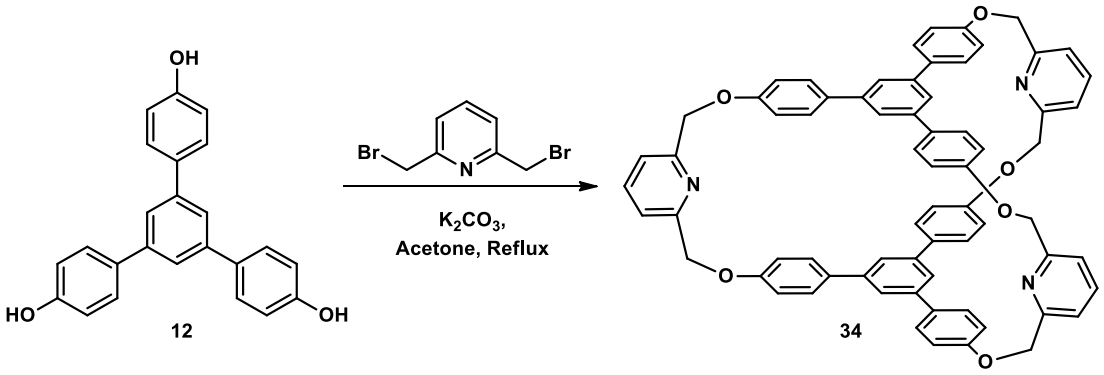

Scheme 17. *Synthesis of cryptand **34**.*

The reaction was performed in identical conditions with compound **33**, by using the same concentration and reagents. An attempt on isolating compound **34** on column chromatography was made, however the purity of the final compound was not satisfactory, the purification proving to

be more challenging than that of the 1,3,5-triazine-based counterpart. Nonetheless, an ES(+)-MS was performed at room temperature on the fraction with the highest purity confirming the presence of the target compound with a molecular peak at m/z = 1018.38 $[M+H]^+$. Moreover, the spectrum displays an additional molecular peak at m/z = 1056.33 $[M+K]^+$ suggesting that the cryptand might have potential applications in encapsulating potassium and other metal ions. ^{1}H NMR spectroscopy further confirmed the structure of the target compound by displaying the expected number and pattern of resonances. Unfortunately, the purity of the isolated product was not adequate for complexation studies, but further purifications will be made and if the results are promising, a comparison with cage molecule **33** should provide an interesting insight regarding the binding abilities of this type of cryptands.

Chapter 4. APPLICATIONS

4.1. Investigations on cryptand's 33 properties towards new mechanically interlocked cryptand-macrocycle assemblies

The ever-growing interest in the synthesis of interlinked molecules, along with the increased efficiency in the use of chemical templation, prompted us to investigate the applicability of cryptand **33** (**Chart 3**) in accessing higher order assemblies with increasingly sophisticated molecular topologies. Therefore, we designed new supramolecular architectures based on the cage molecule **33,** which, by intertwining one or more macrocycles inside the cavity or around the connecting bridges of the cryptand, would lead to new macrocycle-cryptand catenanes. The rapid development of the active metal template (AMT) approach towards mechanically interlocked molecules, as well as the ease of synthesis and higher yields, encouraged us to apply this method in the development of the new interlocked architectures.

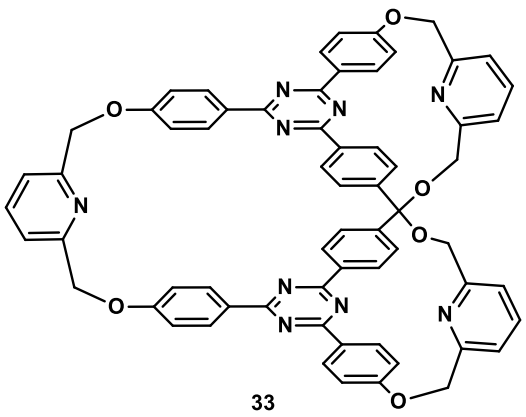

Chart 3. *Cryptand **33** as starting point for new mechanically interlocked architectures.*

Two types of cryptand-macrocycle supramolecular assemblies were envisioned. The design of the first type (**Chart 4**) relies on entrapping a macrocycle inside the cavity of the cryptand. The macrocycle is assembled from three identical building blocks, more precisely threads bearing an azide and an alkyne at each end. Three Cu^{I} ions coordinated at each of the pyridyl bridges of cryptand **33** along with a complementary azide from one thread and alkyne from the subsequent thread are gathered within the cavity of the cryptand. Not only that the Cu^{I} cation acts as a templation agent, it also mediates the terminal alkyne-azide cycloaddition (CuAAC) reaction, thus resulting in covalently binding the three threads together to form the macrocycle trapped inside the cavity.

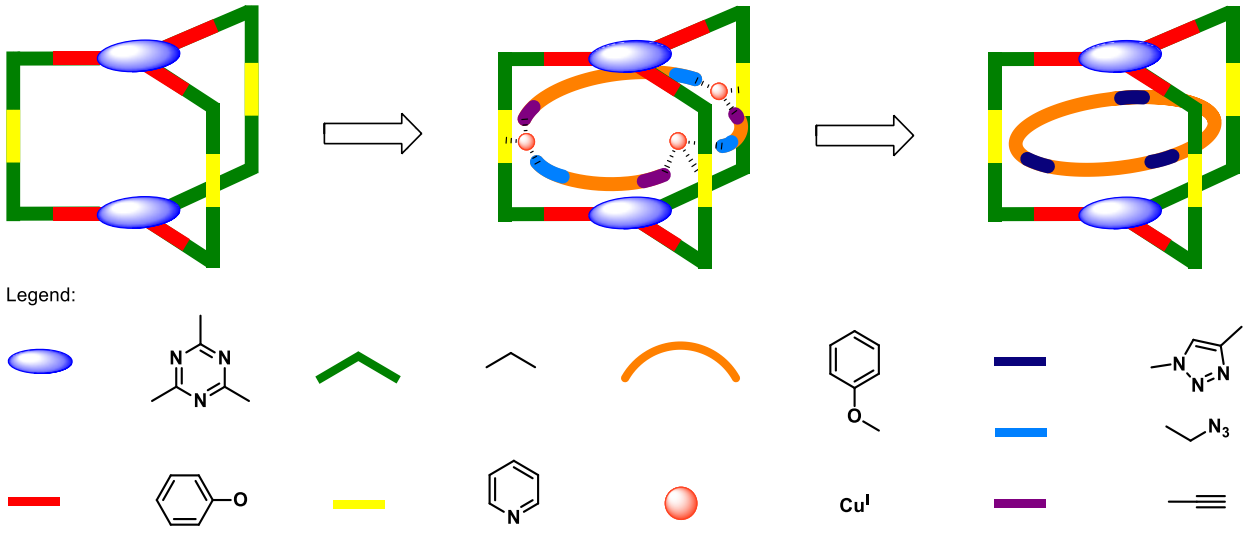

Chart 4. *Cartoon representation of the synthetic approach towards new mechanically interlocked cryptand-macrocycle assemblies.*

The first step towards the synthesis of the interlocked molecular cage resided in the synthesis of the azide-alkyne thread **40** (**Scheme 18**) as a precursor for the trimeric macrocycle.

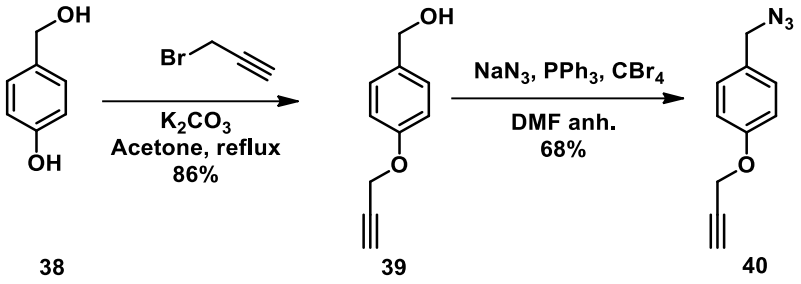

Scheme 18. *Synthesis of azide-alkyne **40**.*

Derivative **40** was prepared using a two-step reaction strategy, starting from the commercially available 4-hydroxybenzyl alcohol. The first step was undertaken by reacting the propargyl bromide with 4-hydroxybenzyl alcohol, following a previously reported procedure[8]. After purification the isolated derivative **39** was employed in the next step of the synthetic procedure, which implied a one pot reaction beginning with the bromination of the alcohol group, followed by the nucleophilic substitution of the bromine group with an azide moiety.

Following the isolation of the target azide-alkyne **40**, the investigation concerning the potential of cryptand **33** in accessing higher order supramolecular architectures was undertaken. Thereby, the newly obtained derivative **40** was employed in a copper catalyzed azide–alkyne cycloaddition (CuAAC) reaction along with the cage molecule **33** in order to afford a trimeric macrocycle trapped inside the cryptand's cavity (**Scheme 19**).

[8] C. Wang, X. Zheng, R. Huang, S. Yan, X. Xie, T. Tian, S. Huang, X. Weng, X. Zhou, *Asian J. Org. Chem.* **2012**, *3*, 259.

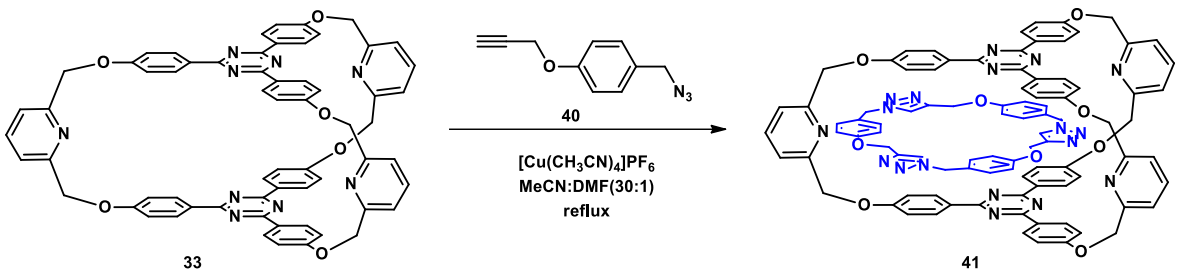

Scheme 19. *Active metal template reaction between cryptand **33** and azide-alkyne **40**.*

An APCI(+)-MS spectrum (**Figure 4**) performed on the crude product, before demetallation, revealed three characteristic peaks at *m/z* = 1460.43, *m/z* = 1647.51 and *m/z* = 1834.58 corresponding to [(**33**)(**40**)$_2$Cu]$^+$, [(**33**)(**40**)$_3$Cu]$^+$and[(**33**)(**40**)$_4$Cu]$^+$ adducts, which suggests that the cage molecule **33** is able to form complexes with the azide-alkyne **40** and thus participating in the CuAAC reaction. No adducts between **33** and a single molecule of **40** were found.

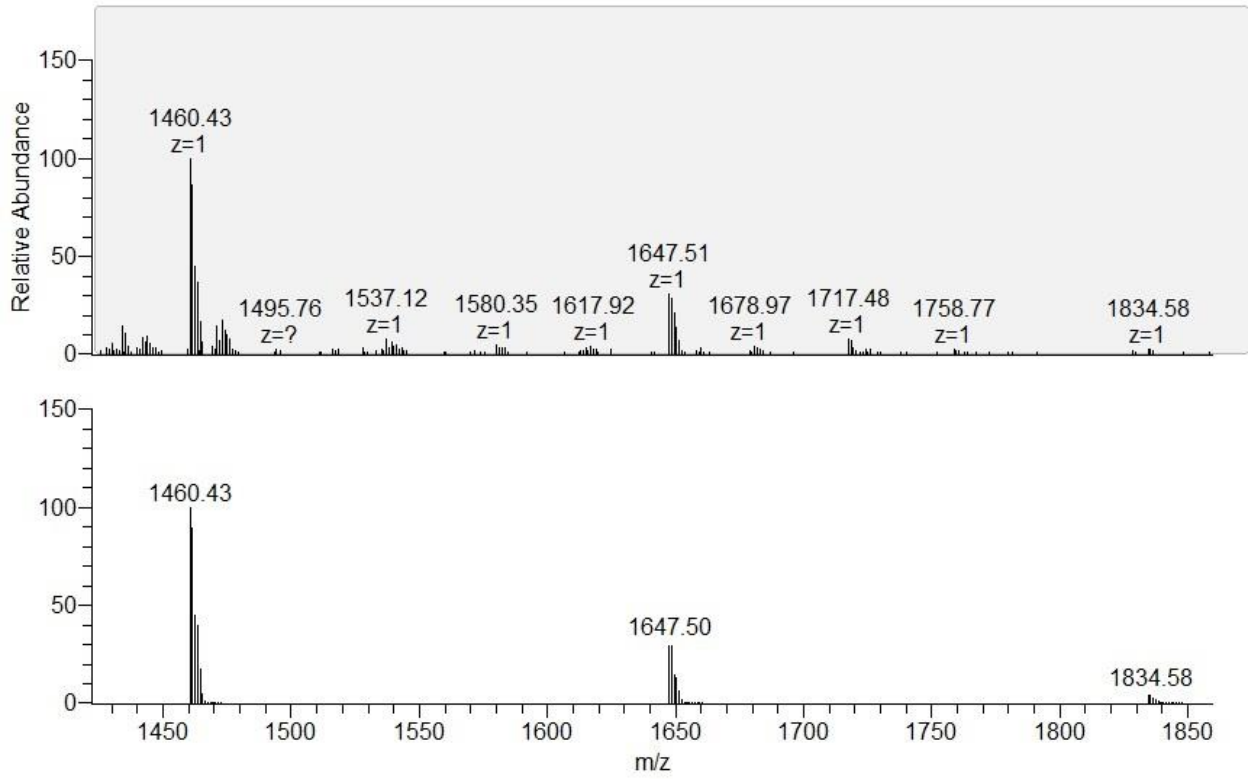

Figure 4. *APCI(+)-MS spectra displaying the [(**33**)(**40**)$_2$Cu]$^+$, [(**33**)(**40**)$_3$Cu]$^+$and[(**33**)(**40**)$_4$Cu]$^+$ adducts. Comparison of the experimental spectra (top) and simulated isotopic patterns (bottom).*

After washing the crude product with a saturated solution of EDTA, to remove any traces of copper, another APCI(+)-MS experiment was performed. The resulting spectrum (**Figure 5**) displayed the molecular peaks corresponding to the dimeric, trimeric and tetrameric structures resulted from **40**. Therefore, the spectrum reveals a peak at *m/z* = 375.16 corresponding to $[(\mathbf{40})_2+H]^+$ and two more peaks at *m/z* = 562.23 and *m/z* = 749.31 corresponding to $[(\mathbf{40})_3+H]^+$ and $[(\mathbf{40})_4+H]^+$ respectively. However, no interactions between these three newly formed compounds and cryptand **33** were found.

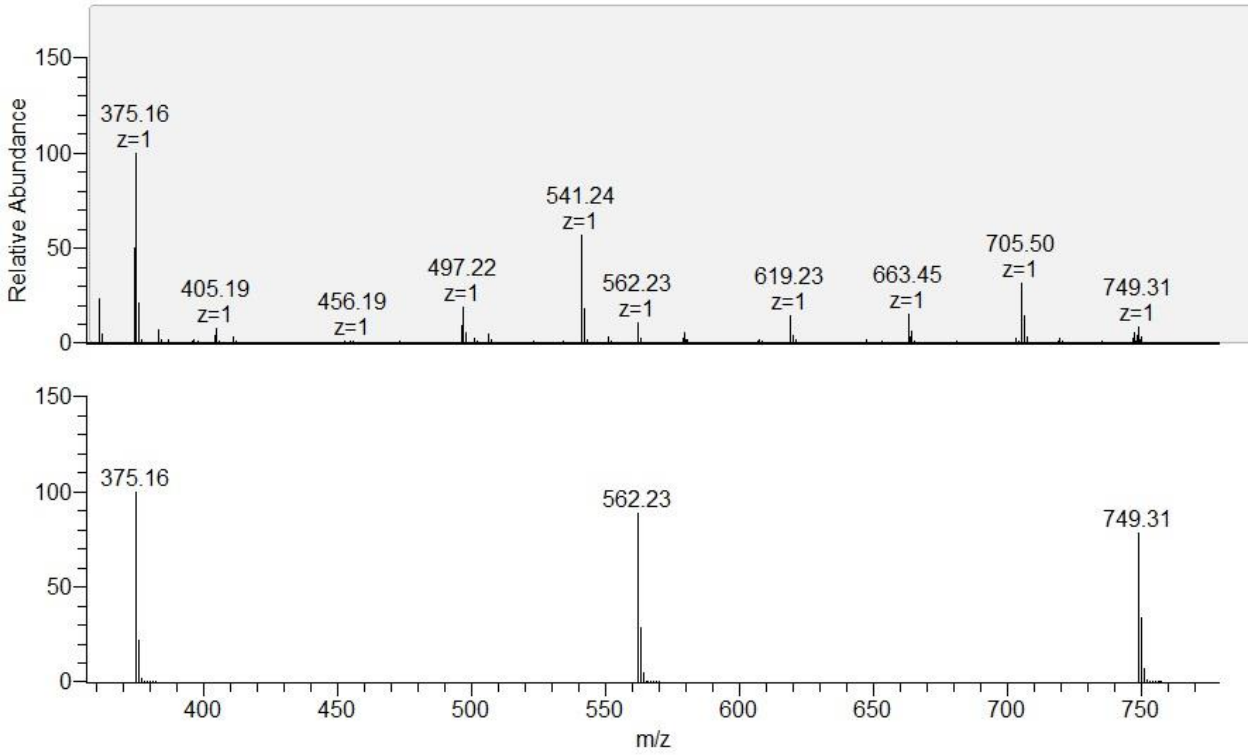

Figure 5. *APCI(+)-MS spectra displaying the $[M+H]^+$ molecular ions of the dimeric, trimeric and tetrameric structures resulted from azide-alkyne **40**. Comparison of the experimental spectra (top) and simulated isotopic patterns (bottom).*

The ^{1}H NMR spectra performed on the crude product showed no trace of the signal corresponding to the proton from the acetylenic group, suggesting that the newly formed compounds present a macrocyclic structure, otherwise, any other alternative polymeric structure would display at least one unreacted acetylenic group.

Figure 32 presents a comparison between ^{1}H NMR spectra of azide-alkyne **40** (top) and the crude product resulted from the reaction (bottom), displaying the absence of the signal corresponding to the proton from the acetylenic group after the reaction with the cryptand **33** and the appearance of a singlet at 6.8 ppm corresponding to the proton from the triazole unit.

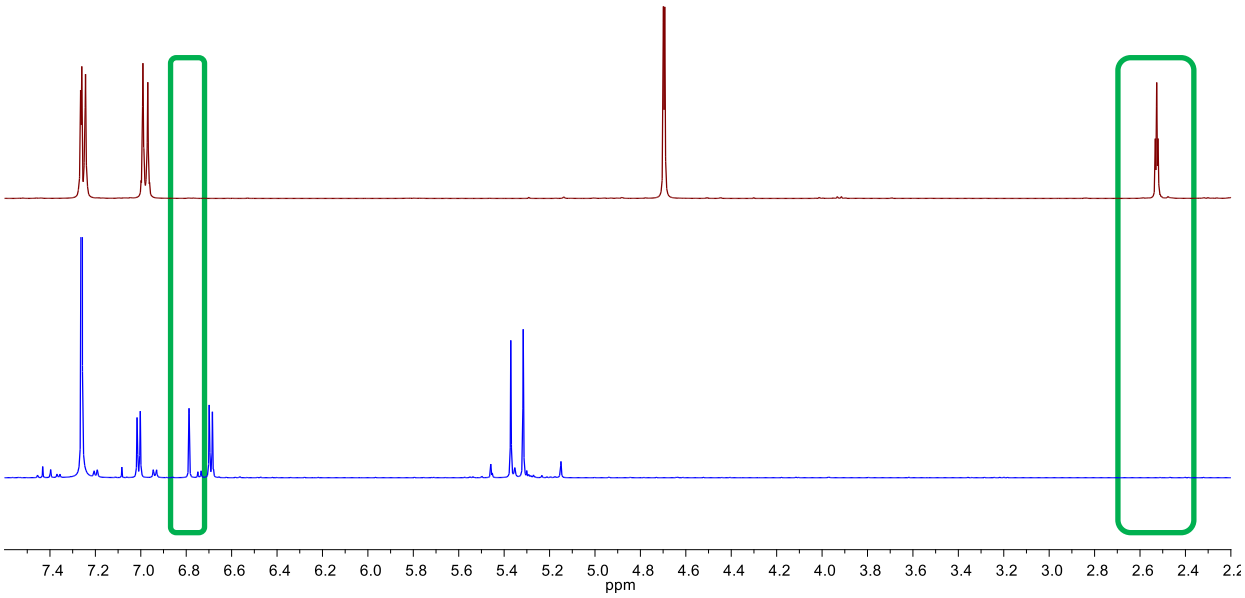

Figure 32. *Comparison between ^{1}H NMR ($CDCl_3$, 600 MHz) spectra of derivatives **40** (top) and the crude product resulted from the CuAAC reaction of **40** with cryptand **33** (bottom).*

Although the reaction did not yield the desired mechanically interlocked compound, the result is particularly interesting due to its application of the recently developed active metal template (AMT) strategy in obtaining well-defined compounds like the previously mentioned dimer, trimer and tetramer. This aspect provides some interesting perspectives for future research and requires further investigation.

4.2. Investigations on cryptand's 33 properties towards new crypto-catenanes

The second type of cryptand-macrocycle assembly (**Chart 5**) requires the intertwining of one or more macrocycles around the pyridyl bridges of the cryptand. To achieve this, a thread, decorated with an azide at one end and a terminal alkyne at the other, would be employed in a macrocyclization reaction which closes the ring around the cryptand's bridges, leading to a crypto-

catenane with one or more rings intertwined with the cryptand. Once again, a Cu^{I} ion would be employed to act both as template and as catalyst for the CuAAC reaction which locks the macrocycle around the cryptand's bridging units and thus forming the crypto-catenane.

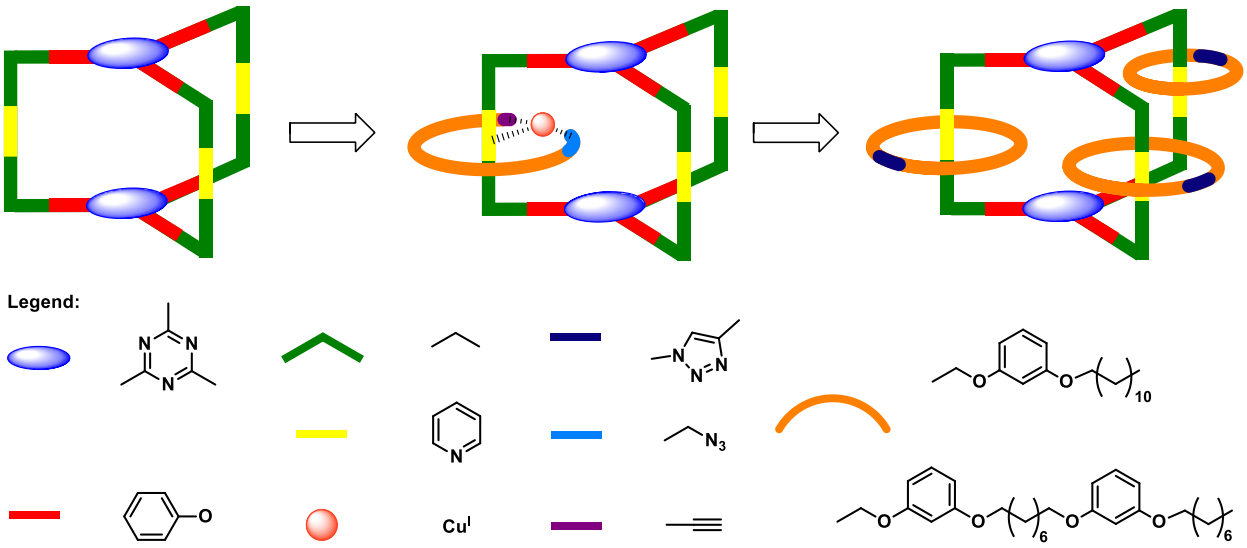

Chart 5. *Cartoon representation of the synthetic approach towards new crypto-catenanes.*

Two types of azide-alkyne threads were designed for this purpose (**Chart 6**): a shorter thread, bearing one resorcinol unit and two alkyl chains and a longer one constructed from two resorcinol units linked by a flexible bridge and two alkyl chains decorated with azide and terminal alkyne moieties.

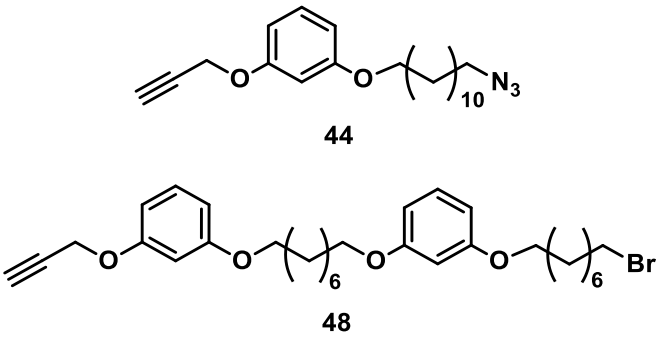

Chart 6. *Target azide-alkynes.*

Synthesys of azide-alkyne thread 44

The synthesis of the first azide-alkyne thread consisted in a three-step strategy, starting from the resorcinol unit and inserting, with each step, suitable building blocks bearing terminal alkyne and azide groups, as shown in **Scheme 20**.

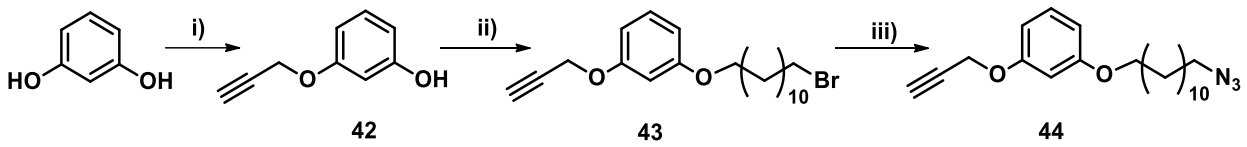

Scheme 20. *Synthesis of the new resorcine-based ligands: i) propargyl bromide, K_2CO_3, acetone, reflux, 30 %; ii) 1,12-dibromododecane, K_2CO_3, acetone, reflux, 29 %; iii) sodium azide, acetonitrile, reflux, 98 %.*

The first step in the synthetic approach consisted in the decoration of benzene-1,3-diol with a triple bond, *via* a substitution reaction, using propargyl bromide as electrophilic reagent and K_2CO_3 as base to generate the nucleophile. In order to avoid the formation of the disubstituted derivative, a stoichiometric excess of resorcinol was used and the electrophile was added dropwise. Subsequently, the de-symmetrised derivative **42** was subjected to another substitution reaction using the same conditions as in the first step, but employing 1,12-dibromododecane instead of propargyl bromide. In this step an excess of electrophilic reagent was used to prevent the attack of the nucleophile to both electrophilic centres having bromine atoms as leaving groups and thus obtaining a dimer instead of the desired monomer **43**. The excess of 1,12-dibromododecane was removed by column chromatography, affording compound **43** as a pure product. Moving further to the next step of the synthetic approach, treatment of the brominated compound **43** with sodium azide afforded the corresponding azide derivative **44** in almost quantitative yield. All synthesized derivatives **42**, **43** and **44** were characterized by nuclear magnetic resonance (NMR) and mass spectrometry.

Synthesys of azide-alkyne thread 48

An alternative method explored while investigating the synthesis of crypto-catenanes required the use of a longer thread that allows a more facile intertwining around the pyridyl bridges of the cryptand. In this regard, we prepared a ligand bearing two resorcinol units linked by a

flexible alkyl chain which was subsequently decorated with a terminal acetylene block on one side and an azide group at the other end (**Scheme 21**).

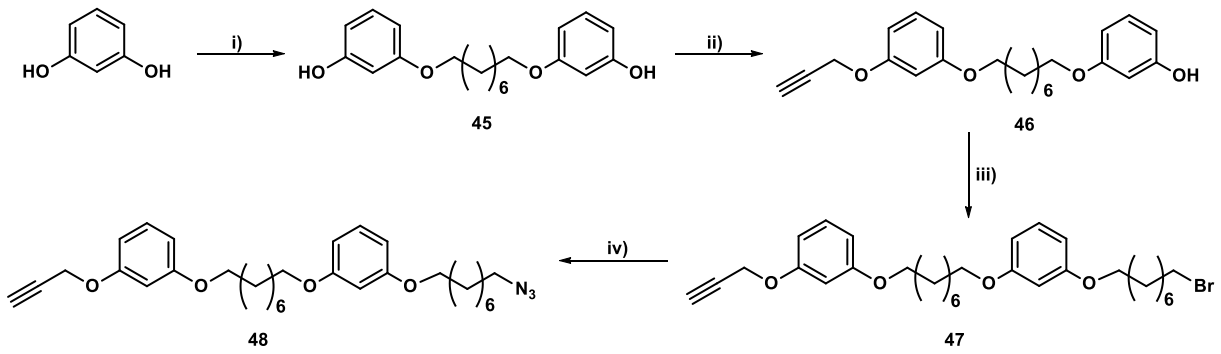

Scheme 21. *Synthesis of the new resorcine-based ligands **45**-**48**: i) 1,8-dibromooctane, K_2CO_3, acetone, reflux, 58 %; ii) propargylbromide, K_2CO_3, acetone, reflux, 54 %; iii) 1,8-dibromooctane, K_2CO_3, acetone,reflux, 27 %; iv) sodium azide, acetonitrile, reflux, 65 %.*

1,8-dibromooctane was chosen as linker between the two resorcinol moieties and were collectively employed in a disubstitution reaction which, after purification on column chromatography, afforded compound **45** in 58 % yield. Next, the isolated derivative **45** was subjected to a subsequent reaction with propargyl bromide, which provided the non-symmetrical compound **46** in 54 % yield. The obtained derivative **46** was treated in the next step with 1,8-dibromooctane with the aim of introducing a bromine group in the molecule and to further extend the thread's length. In the following step, the conversion of bromine to azide was attained by reacting the newly obtained compound **47** with sodium azide in acetonitrile at reflux, allowing the target compound **48** with a 65 % yield. The structure of all synthesized derivatives **45**-**48** was characterized by nuclear magnetic resonance (NMR) spectroscopy and mass spectrometry.

Towards new mechanically interlocked molecular cages. The active metal template (AMT) approach.

Following the isolation and characterization of the target threads **44** and **48**, the newly obtained azide-alkynes were exploited, along with cryptand **33**, in an effort to investigate the efficiency of the active metal template (AMT) approach in synthesizing more intricate mechanically interlocked molecules.

In the first attempt, compounds **33** and **44** were employed in a CuAAC 'click' reaction, with the aim of attaining either the single-, double- or the triple-threaded cryptocatenanes **49**, **50** and **51** (**Scheme 22**).

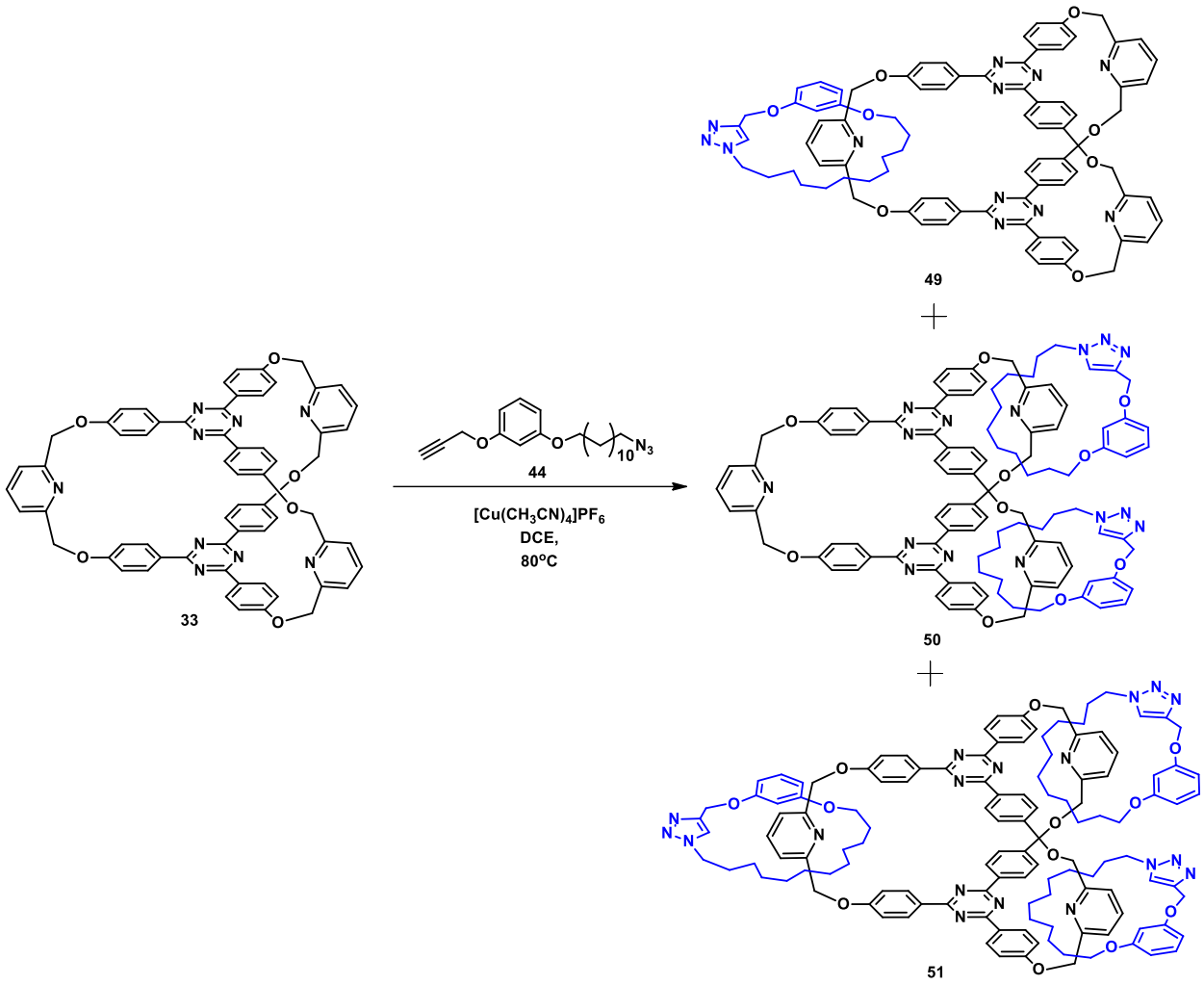

Scheme 22. *Synthetic procedure for obtaining single-, double- or the triple-threaded cryptocatenanes **49**, **50** and **51**.*

The reaction occurred in degassed 1,2-dichloroethane (DCE) with tetrakis acetonitrile copper(I) hexafluorophosphate providing the metal required for the AMT synthesis. Once the TLC monitoring showed no traces of the starting compounds, the reaction was stopped and the product was subjected to a demetallation procedure using a solution of EDTA and K_2CO_3.

An ES(+)-MS spectrum performed on the crude of the reaction revealed the possible formation of a complex between cryptand **33** and a dimeric structure resulted from the CuAAC

reaction of azide-alkyne **44** by displaying the $[\mathbf{33}\cdot(\mathbf{44})_2\cdot H]^+$ molecular peak at *m/z* = 1739.84. Moreover, peaks found at *m/z* = 1761.83 $[\mathbf{33}\cdot(\mathbf{44})_2\cdot Na]^+$ and *m/z* = 1777.80 $[\mathbf{33}\cdot(\mathbf{44})_2\cdot K]^+$ reveal the formation of complexes with sodium and potassium cations (**Figure 5**).

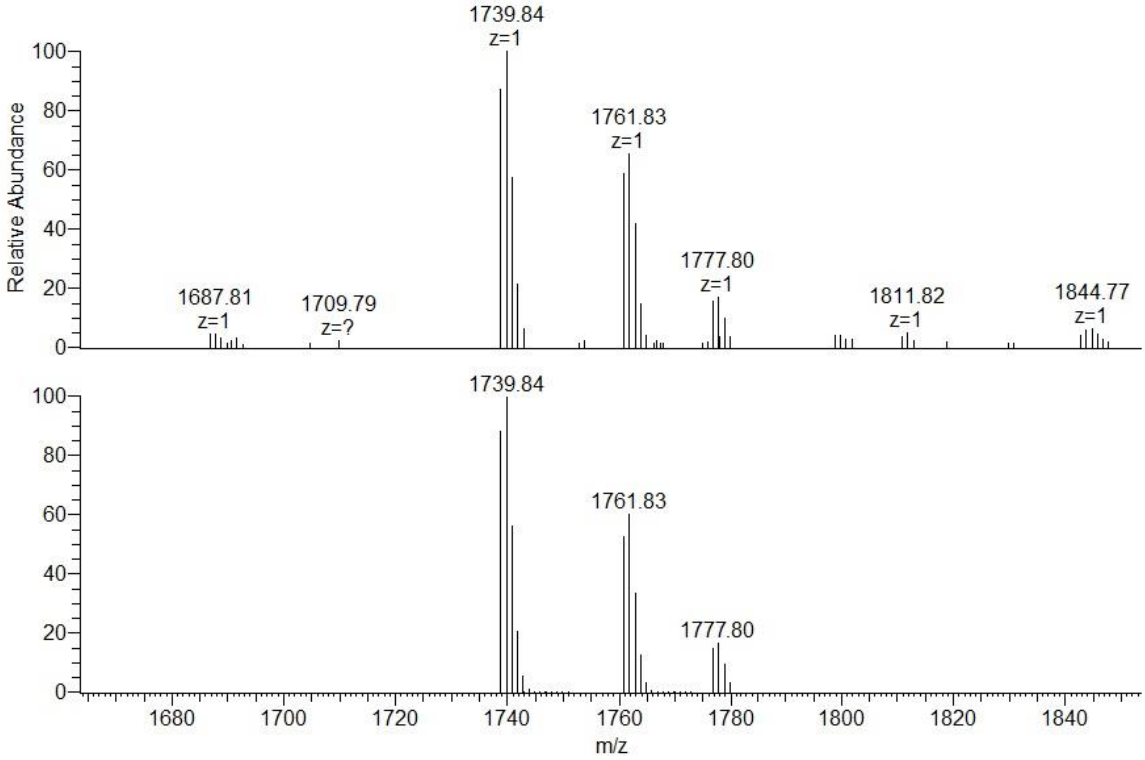

Figure 5. *ES(+)-MS spectrum of the complex between cryptand **33** and the dimeric structure resulted from azide-alkyne **44**. Comparison of the experimental spectra (top) and simulated isotopic patterns of* $[\mathbf{33}\cdot(\mathbf{44})_2\cdot H]^+$, $[\mathbf{33}\cdot(\mathbf{44})_2\cdot Na]^+$ *and* $[\mathbf{33}\cdot(\mathbf{44})_2\cdot K]^+$.

The ^{1}H NMR experiments performed on the same product revealed no traces of the triplet belonging to the proton from the acetylenic group, suggesting that the azide-alkyne was fully consumed in the reaction, while a new singlet (most probably from the newly formed triazole) appeared in the aromatic region. This finding helped us eliminate the hypothesis regarding an alternative formation of a complex between cryptand **33** and the two unreacted azide-alkynes, which would display peaks at the same *m/z* values. Unfortunately, after several purification attempts, the product could not be isolated. Therefore, with the data gathered so far, two possible structures might be envisioned: the cryptand and two separated macrocycles (**Chart 7a**) or the cryptand and a dimeric macrocycle (**Chart 7b**) in either mechanically interlocked configuration,

as pictured, or in other alternative forms such as cryptand-macrocycle complexes. The final verdict on the actual structure can only be given with the aid of X-ray crystallography, however, despite the efforts, no crystals suitable for X-ray analysis could be obtained so far.

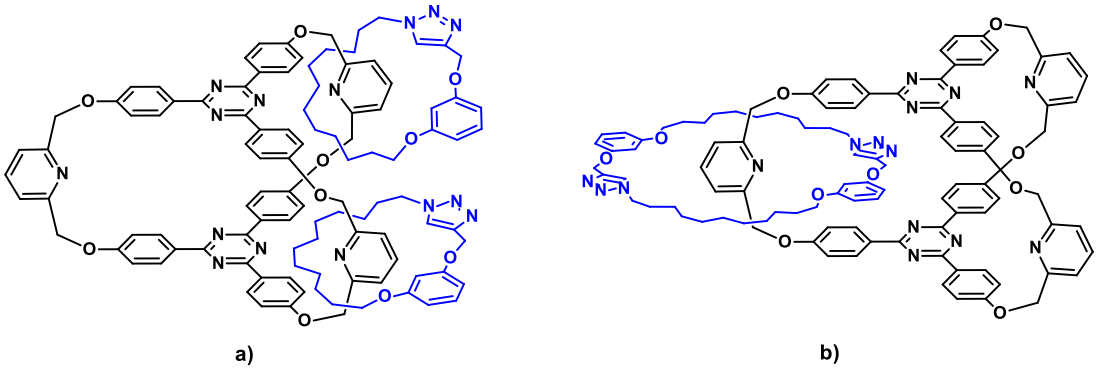

Chart 7. *Possible structures resulting from the active metal template reaction between cryptand **33** and azide-alkyne **44**.*

A second strategy, this time involving a longer thread, was also investigated. The approach consisted in employing derivative **48** along with cryptand **33** in an AMT procedure, with the aim of synthesizing the single-, double- or triple-threaded crypto-catenanes **52**, **53** and **54** as shown in **Scheme 23**.

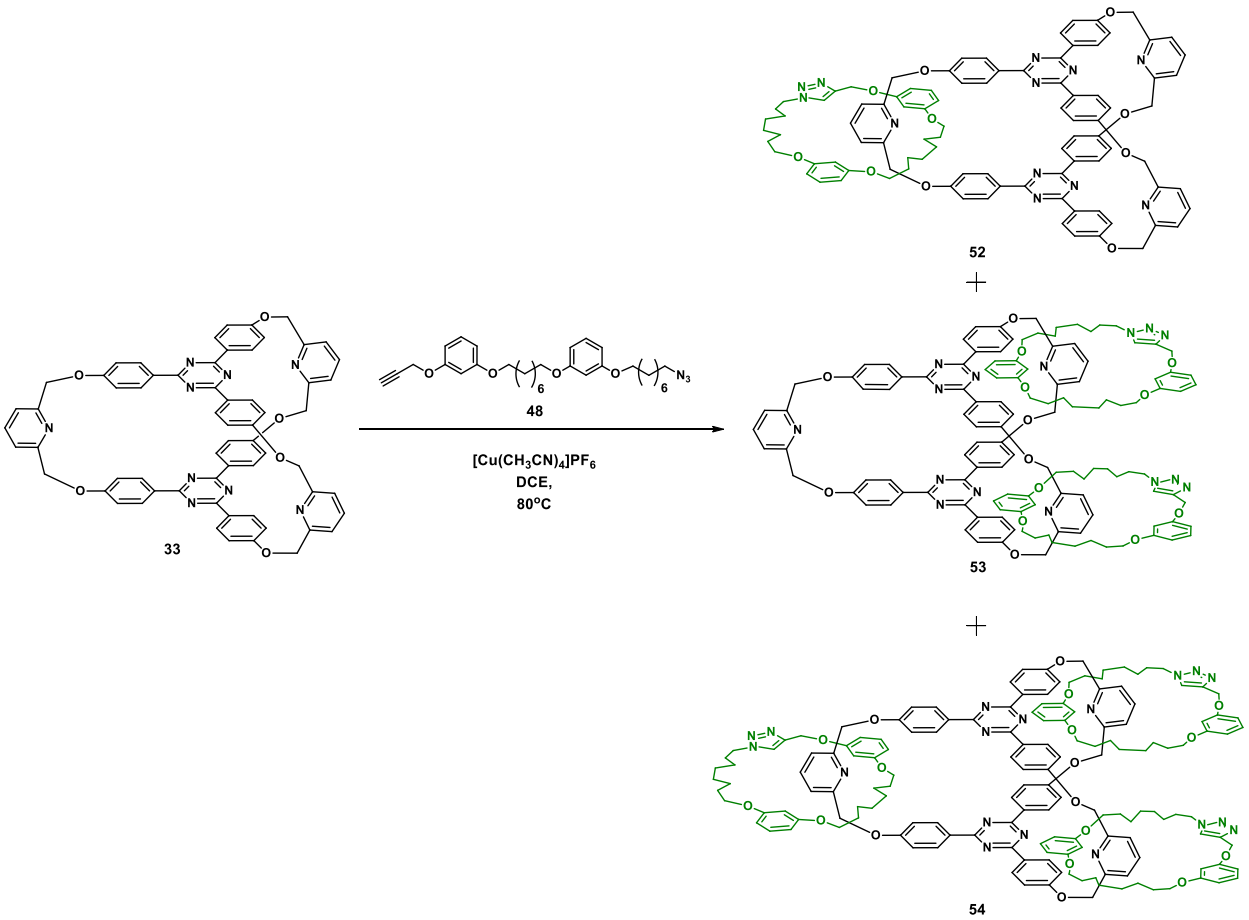

Scheme 23. *Synthetic conditions for preparing crypto-catenanes like **52**, **53** and **54**.*

The reaction was performed in similar conditions with the previously described attempt at obtaining crypto-catenanes **49**-**51**, using degassed 1,2-dichloroethane (DCE) as solvent and tetrakis acetonitrile copper(I) hexafluorophosphate as catalyst. After completion, the crude of the reaction was washed with a solution of EDTA and K_2CO_3 to remove any traces of metal.

Curiously enough, the ES(+)-MS (**Figure 6**) spectrum performed on the obtained product, yielded similar findings to those obtained in the synthesis of crypto-catenanes **49**-**51**. The spectrum displays a peak found at *m/z* = 2068.01 which is associated to the complex between cryptand **33** and a dimeric structure resulted from the azide-alkyne **48**.

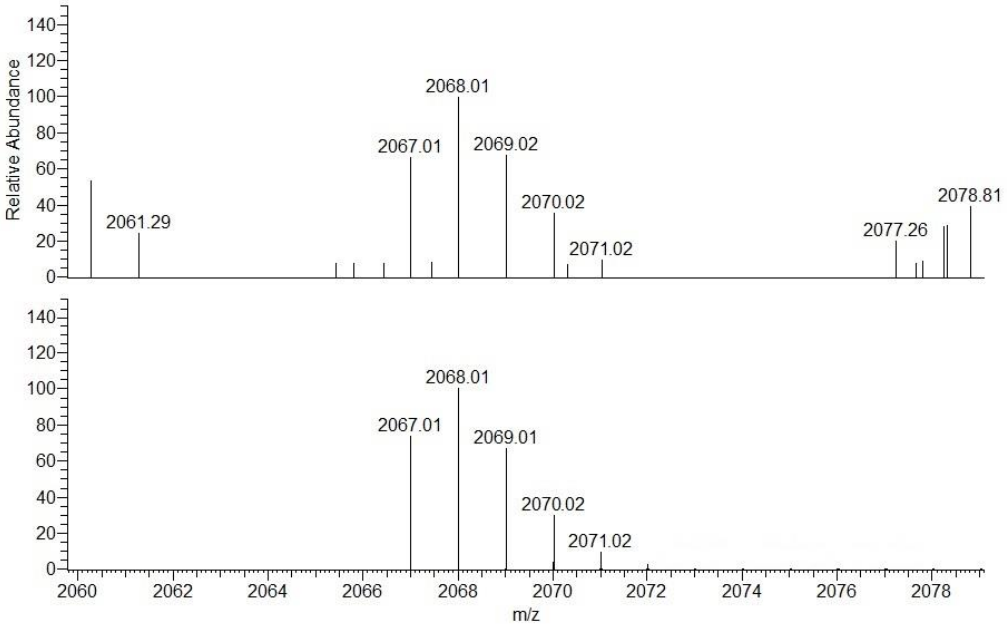

Figure 6. *ES(+)-MS spectrum (fragment) depicting the complex between cryptand **33** and the dimeric structure resulted from azide-alkyne **48**. Comparison of the experimental spectra (top) and simulated isotopic patterns (bottom).*

Once again, the proposed structures, based the data gathered so far, could be composed of one cryptand and two separated macrocycles (**Chart 8a**) or the cryptand and a dimeric macrocycle (**Chart 8b**) in either mechanically interlocked configuration, as pictured, or in other alternative forms such as cryptand-macrocycle complexes.

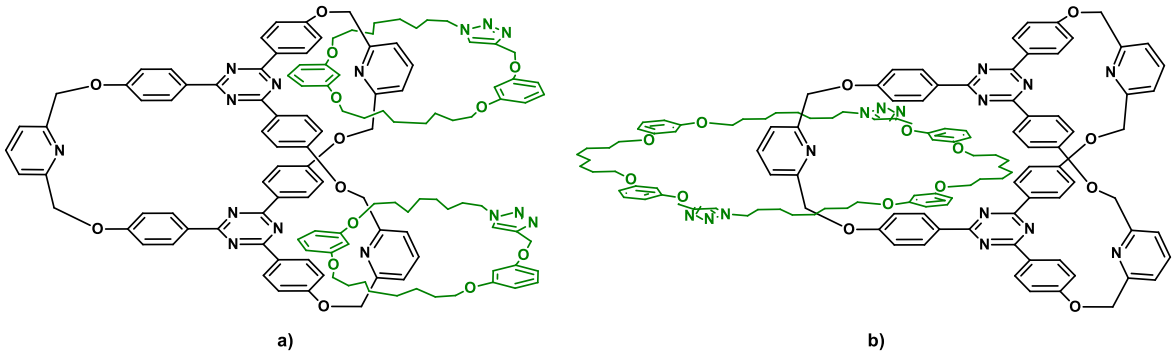

Chart 8. *Possible structures resulting from the active metal template reaction between cryptand **33** and azide-alkyne **48**.*

Unfortunately, the compound proved impossible to isolate, despite the subsequent purification efforts. As with the case of compounds **49**-**51**, the final structure of the compound will only be completely confirmed after X-ray experiments. To this date however, no suitable crystals were found in the prepared samples.

Future perspectives

The purification attempts performed on both reactions yielded several non-interlocked macrocyclic molecules (dimeric, trimeric, tetrameric), suggesting that a significant part of the process involving the formation of the triazole and, along with it, the conversion of the azide-alkyne thread into the macrocyclic structure, does not take place around the cryptand's bridges, except for maybe a small fraction. This might imply that the reaction occurs similar to the reactions applied in the statistical method[9] in which the formation of the interlocked compound relies more on probability rather than the actual pre-organization of the components. A solution to this problem might be provided by a more flexible pyridyl bridge. The previously described cryptand **20** (**Chart 9**) was specifically designed for this purpose having an additional methylene group that makes the junction between the aromatic unit and the oxygen atom. This increases the flexibility of the pyridyl bridge and places the oxygen atoms in a more favorable position, allowing them to participate in the coordination of the copper ion[10] to the pyridyl bridge and thus stabilizing the whole complex and gathering all the loose threads of the azide-alkyne chain together, placing them in a more favorable position. Moreover, having only one pyridyl bridge reduces the number of possible interlocked structures resulted from the CuAAC reaction, simplifying the isolation procedures. Therefore, further investigations regarding the applicability of cryptand **20** in accessing crypto-catenanes should provide some interesting perspectives for future research.

[9] A. Godt, *Eur. J. Org. Chem.* **2004**, *8*, 1639.

[10] S. M. Goldup, D. A. Leigh, T. Long, P. R. McGonigal, M. D. Symes, J. Wu, *J. Am. Chem. Soc.* **2009**, *131*, 15924.

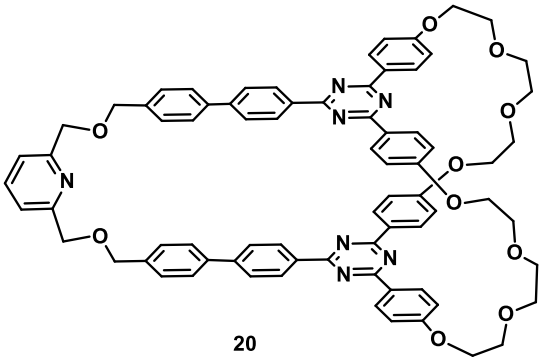

Chart 9. *Cryptand **20** bearing only one pyridyl bridge and with more conveniently-placed oxygen atoms.*

Although the final structures of both compounds **50** and **53** are yet to be confirmed, the reactions provided some particularly interesting insights about the possible formation of mechanically interlocked cryptand-macrocycle architectures, as well as laying the foundation for future research in this fascinating newly born field of crypto-catenanes.

4.3 Complexation properties of cryptands 21, 22 and 23

The previously synthesized cryptands **21-23** (**Chart 10**; for more information see **Chapter 3.2.1**) were subjected to investigations regarding their complexation ability towards alkali metal cations, as well as organic ammonium ions such as the dication of 1,5-diaminonaphthalene. In order to examine the capability of cryptands **21-23** to accommodate the designated guests, binding studies were performed using ES(+) MS and ^{1}H NMR spectroscopy.

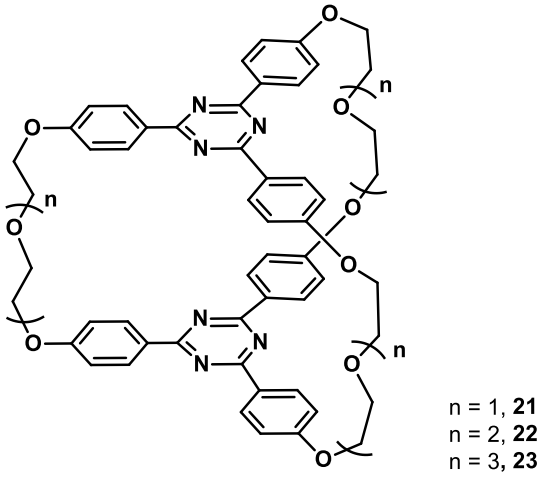

Chart 10. *General structure of cryptands **21-23**.*

The ES(+) MS studies were conducted with the aim of investigating the interaction between the synthesized cryptands **21-23** and the alkali metal ions as well as the diprotonated 1,5-naphthylenediamine, while the ^{1}H NMR experiments were performed in order to study the formation of the complex between cryptand **23** and the dication of 1,5-naphthylenediamine.

The affinity towards alkaline-metal cations was assessed by means of mass spectrometry, employing equimolar amounts of hosts **21**, **22** or **23**, combined with a mixture of the cations from the first group, Li^+, Na^+, K^+, Cs^+ (LiCl, $NaIO_4$, KSCN and $1/2xCs_2CO_3$) in competitive complexation experiments.

The results reveal that the cryptand with the shortest bridges (**21)** displays the highest abundance of the protonated species $[M+H]^+$, while the larger hosts **22** and **23** show the complexes with K^+ as the base peak. The $[M+Li]^+$ peak is present in the spectra performed on compounds **21** and **22**, exhibiting small intensities (8% for **21** and 4% for **22**), while in the case of compound **23** this peak is completely missing, suggesting a decrease of affinity for Li^+ cations as the bridges of the cage molecules grow longer. The $[M+Cs]^+$ peak on the other hand is missing from the spectrum of host **21** and it is present in the spectra of **22** (11%) and **23** (4%), while the peak corresponding to the $[M+Na]^+$ species is present in all three cases, with a slightly higher intensity in the case of compound **21** (39% for **21** and 30% for **22** and **23**). For exemplification purposes, a comparison of the ES(+)-HRMS spectrum performed on compound **23** in a mixture of equivalent amounts of LiCl, $NaIO_4$, KSCN, Cs_2CO_3 (4.2×10^{-6} mM in methanol) and the simulated isotopic patterns of [**23**·H^+], [**23**·Na^+], [**23**·K^+] and [**23**·Cs^+] adducts is displayed in **Figure 7**. The spectrum shows the protonated ion $[M+H]^+$ at *m/z* = 1189.52 and the $[M+Na]^+$ adduct at *m/z* = 1211.50, while the peaks corresponding to the $[M+K]^+$ and $[M+Cs]^+$ are present at *m/z* = 1227.47 and *m/z* = 1321.42, respectively.

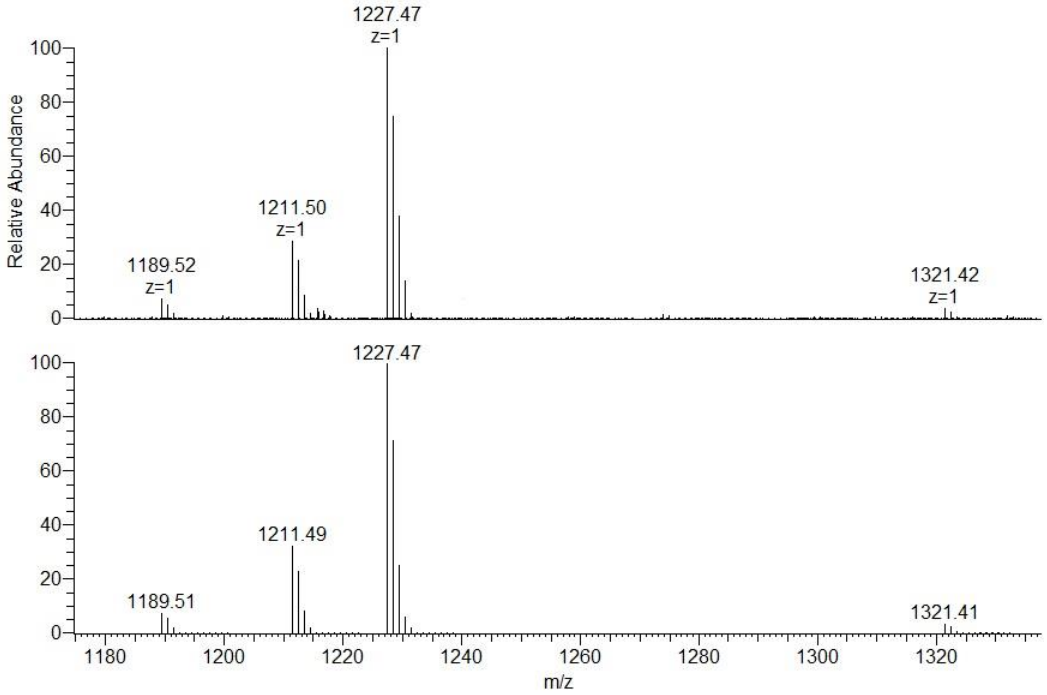

Figure 7. *ES(+)-HRMS spectra of **23** in presence of equivalent amounts of LiCl, $NaIO_4$, KSCN, Cs_2CO_3 4.2 x 10^{-6} mM in methanol (top). Comparison of the experimental spectra (top) and simulated isotopic patterns of [**23**·H^+], [**23**·Na^+], [**23**·K^+] and [**23**·Cs^+] adducts (bottom).*

Investigation of binding characteristics between cryptand **23** as host and 1,5-naphthalenediamine (NA) as guest was undertaken by using samples containing 4.2x10^{-3} mM solutions of **23** and NA in $CHCl_3$/MeCN 1:4 v/v with 0.1% TFA. The ES(+)-MS spectrum of the reaction performed at room temperature for 1 h reveals characteristic peaks at *m/z* = 685.23 and *m/z* = 693.22 corresponding to the double charged species [(**23**)·(NA)·Na^+·H^+] and [(**23**)·(NA)·K^+·H^+] as well as peaks corresponding to the double charged species [(**23**)$_2$·(NA)·Na^+·H^+] at *m/z* = 1279.99 and [(**23**)$_2$·(NA)·K^+·H^+] at *m/z* = 1287.98 (**Figure 8** and **Figure 9**).

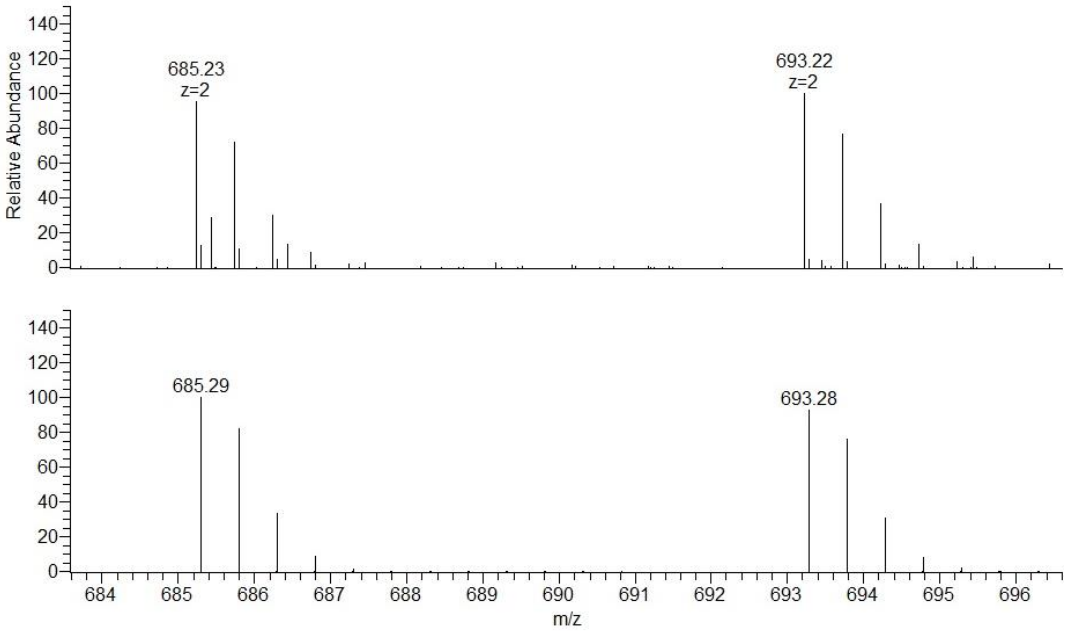

Figure 8. *ES(+)-MS spectra (fragments) of the complexation reaction between **23** and 1,5-naphthalendiamine (**NA**) at rt. Comparison of the experimental spectra(top) and simulated isotopic patterns of the* double *charged species [(**23**)·(NA)·Na^+·H^+] and [(**23**)·(NA)·K^+·H^+] (bottom).*

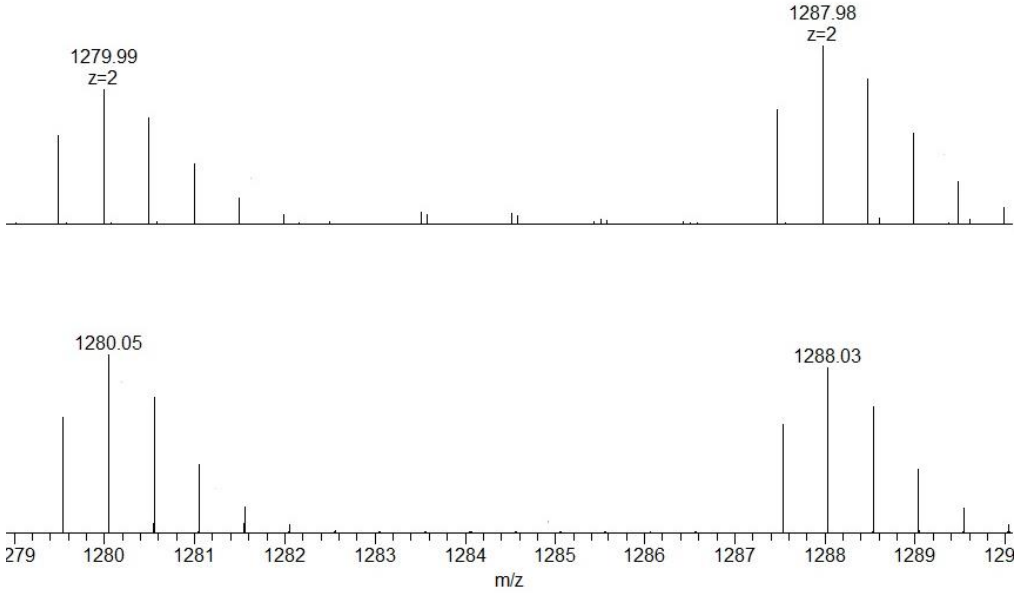

Figure 9. *ES(+)-MS spectra (fragments) of the complexation reaction between **23** and 1,5-naphthalendiamine (**NA**) at rt. Comparison of the experimental spectra(top) and simulated isotopic patterns of the* double *charged species [(**23**)$_2$·(NA)·Na^+·H^+] and [(**23**)$_2$·(NA)·K^+·H^+] (bottom).*

Moreover, the spectrum performed at reflux for 2 h displays three additional peaks corresponding to complexes [(**23**)·(NA)·(TFA)·K^+] at *m/z* = 1499.64, [(**23**)·$(NA)_2$·(TFA)·Na^+] at *m/z* = 1641.70 and [(**23**)·$(NA)_2$·(TFA)·K^+] at *m/z* = 1656.71 respectively (**Figure 10**).

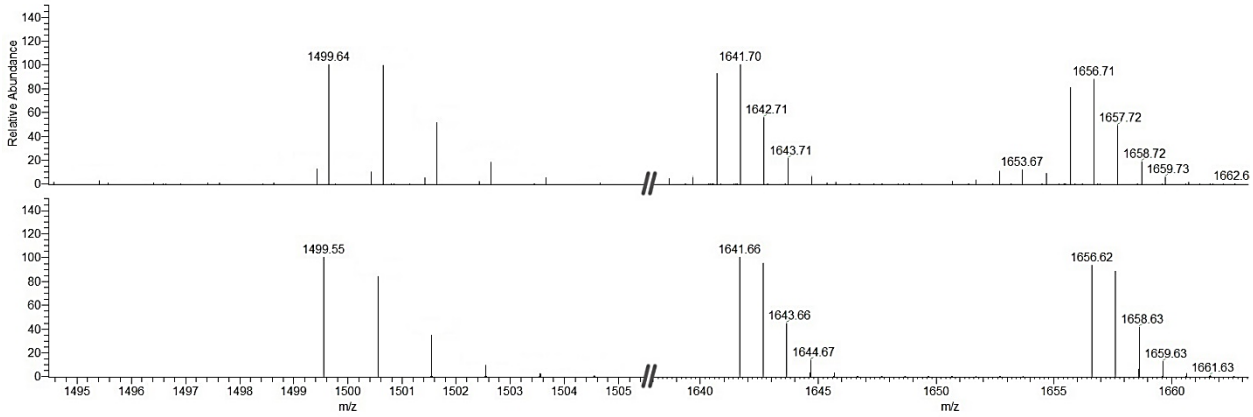

Figure 10. *ES(+)-MS spectra (fragments) of the complexation reaction between **23** and 1,5-naphthalendiamine (**NA**) at reflux. Comparison of the experimental spectra(top) and simulated isotopic patterns (bottom).*

The formation of the complex between cryptand **23** and the dication of 1,5-naphthalenediamine was further confirmed by MS/MS experiments using Collision Induced Dissociation (CID) technique. Therefore, the use of 25-30 eV collision energies on the isolated peaks of the complex yielded the peaks corresponding to [(**23**)·H^+] and/or [(**23**)·Na^+] or [(**23**)·K^+] (**Figure 11**).

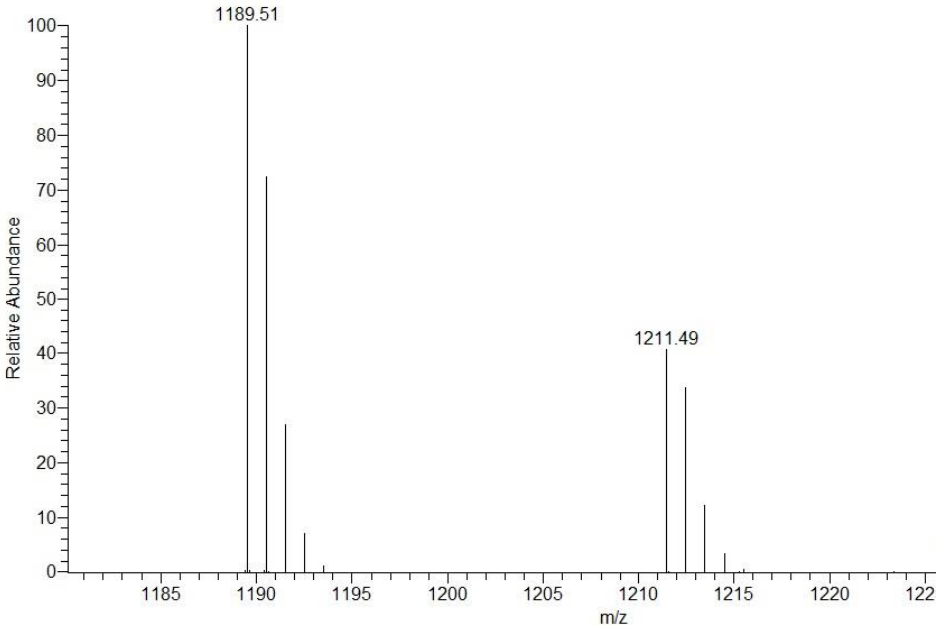

Figure 11. *MS/MS (CID, collision energy 25 eV) of the isolated peak corresponding to [(**23**)·(NA)$_2$·(TFA)·Na$^+$].*

^{1}H NMR investigations were also employed to confirm the formation of the host-guest complex. The experiments were based on the spectra of cryptand **23** (**Figure 12a**), of the diprotonated guest (1,5-naphthalendiamine) (**Figure 12c**) and of a sample exhibiting a host/guest/TFA-d_8 ratio of 1:2.5:5.7 (**Figure 12b**). A comparison between the three spectra revealed the formation of the host-guest adduct, with obvious shifting of the signals in the complex compared to the positions of the signals in the spectra of the isolated host and guest molecules. Therefore, the two doublets assigned to the aromatic protons in the isolated host molecule (δ_{h1}=6.54 ppm; δ_{h2}=7.97 ppm) are brought closer together, with one doublet being moved upfield with 0.05 ppm ($\delta_{h1'}$=6.59 ppm), while the other doublet is shifted downfield with 0.05 ppm in the host-guest complex ($\delta_{h2'}$=7.91 ppm). The signals of the guest molecule (δ_{g1}=7.81 (dd) ppm; δ_{g2}=7.56 (m) ppm) appear more shielded in the host-guest complex, being shifted by 0.14-0.15 ppm ($\delta_{g1'}$=7.67 ppm; $\delta_{g2'}$ =7.41 ppm and 7.46 ppm) (**Figure 12b**). Moreover, the two signals that appear overlapped in the spectrum of the isolated guest are clearly separated in the spectrum of the host-guest complex.

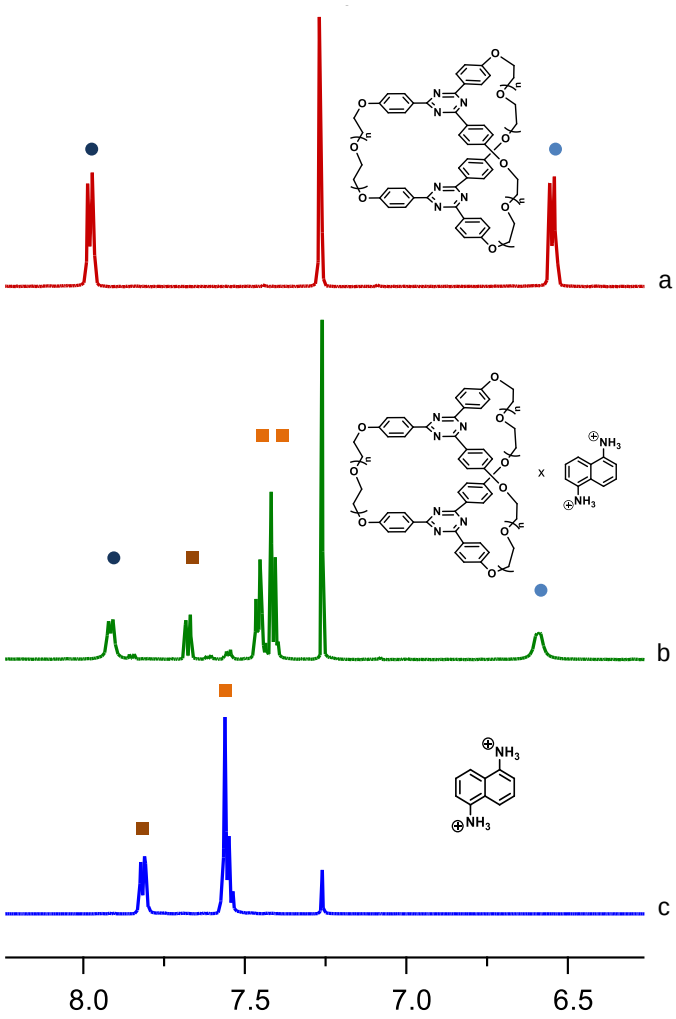

Figure 12. *^{1}H NMR spectra (fragments) of cryptand **23** (a), dication of 1,5-naphthalenediamine (c) and of their host-guest complex (b).*

The stoichiometry of the host-guest complex between cryptand **23** and the diprotonated 1,5-naphthalenediamine (NA) was performed by ^{1}H NMR titration at room temperature. Thirteen NMR samples containing various host/guest ratios were prepared using stock solutions of **23** (2mM) and NA (2mM) in CD_3CN:$CDCl_3$ 4:1 at a final concentration of 2 mM (host [H] + guest [G]). 17 µL of TFA-d were added to each sample.

Since the binding equilibrium has a very fast exchange rate compared to the NMR time scale, the stoichiometry of the host-guest complex was determined by applying a modified Job

plot.[11] Therefore, Δδ x [H] was plotted as y-coordinate and [H]/([H]+[G]) as x-coordinate (**Figure 13**). The obtained data revealed the formation of a host-guest complex at 1:1 binding ratio.

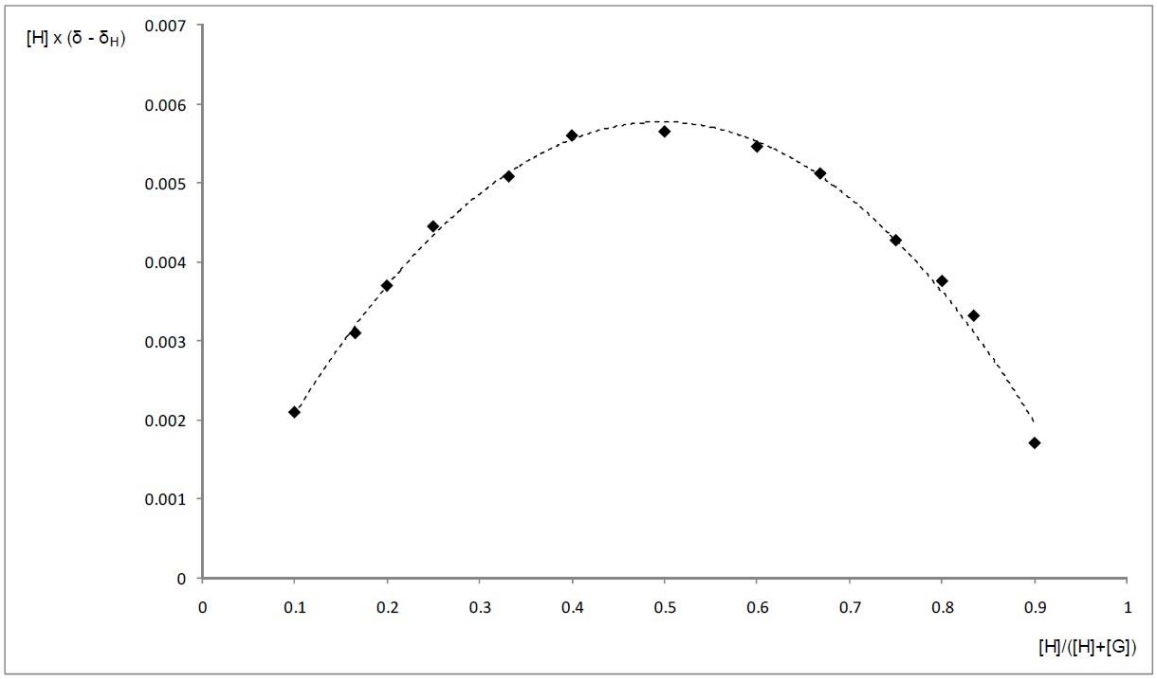

Figure 13. *Job plot of **23**(2mM) with NA (2mM) in $CD_3CN:CDCl_3$ 4:1.*

The association constant was calculated using the relations:

$$\delta = \frac{[H] - x}{[H]} * \delta_H + \frac{x}{[H]} * \delta_c$$

$$K = \frac{x}{([G] - x)([H] - x)}$$

where [H] and [G] are the concentrations corresponding to the total amounts of host (H) and guest (G) and x is the concentration of the formed complex, while δ, δ_H and δ_c are the experimental δ values of the test signal at different host/guest ratios (δ), the δ value of the test signal in the free host molecule (δ_H) and the δ value of the test signal in the complex (δ_c). The δ_c value (8.20499 ppm) was obtained from the linear representation δ = f {[H]/([H]+[G]} (**Figure 14**). The K values were calculated for the H/G ratios 1/1.5 (2.127 x 10^3 L/mol); 1/1 (1.856 x 10^3 L/mol); and 1.5/1 (1.965 x 10^3 L/mol) giving the reported average value K = 1.982±0.13 10^3 L/mol.

[11]K. J. Hirose, *Inclusion Phenom. Mol. Recognit. Chem*. **2001**, *39*, 193.

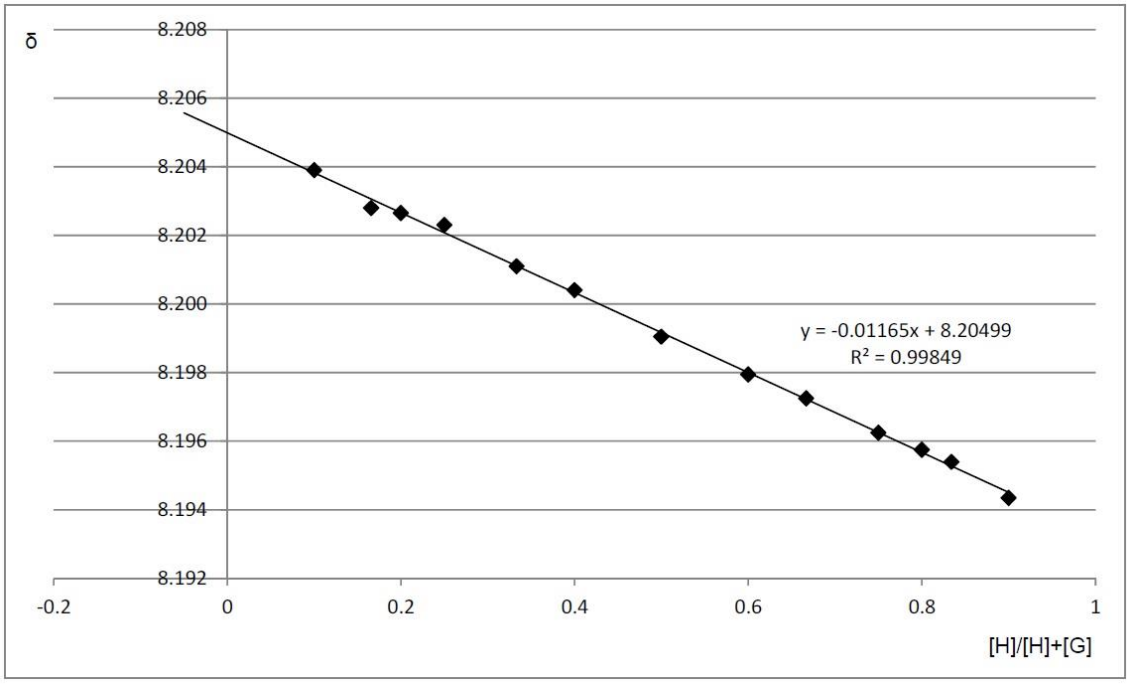

Figure 14. *Determination of δ_c.*

Chapter 5. CONCLUSIONS

The research conducted in this thesis yielded two types of cryptands, as well as several different tripodands and macrocycles which were harnessed in the synthesis of new cage molecules. Furthermore, the properties of some cryptands, as well as their applicability in molecular recognition and in accessing higher order mechanically interlocked architectures was investigated. Therefore:

The decoration of 2,4,6-triaryl-1,3,5-triazine and 1,3,5-triphenyl benzene units yielded five new tripodands, four of which (**24**, **25**, **26**, **28**) were fully characterized and subsequently employed in the synthesis of new cryptands, while tripodand **32** was characterized by mass spectrometry.

The two different synthetic approaches that were investigated, involving one-step or two-step strategies, resulted in the synthesis of six cryptands (**21**, **22**, **23**, **29**, **33**, **34**) displaying a symmetric cavity, amongst which two were characterized by mass spectrometry and four by MS and NMR studies. The structure of cryptand **33** was also confirmed by X-Ray crystallography which revealed a propeller like arrangement with the unit cell containing two molecules, one with

left- and the other one with a right-handed propeller arrangement. This is due to the rotation and orientation of the *p*-phenylene units relative to the 1,3,5-triazine rings. In the case of cryptands **21**, **22** and **23** the two-step procedure proved to be more suitable affording the compounds in higher overall yields.

Eight new macrocycles (**6**, **7**, **13**, **14**, **15**, **16**, **17**, **19**) bearing *m*-xylylene and oligoethylene glycol bridges were investigated as building blocks for new cage molecules with non-symmetrical cavities. The oligoethylene glycol bridges proved to be a more inspired choice compared to the *m*-xylylene bridges, affording macrocycles in higher yields and with a more facile purification.

The desymmetrisation of cryptands, either by employing bridges different from each other, or by attaching distinct central units, afforded three new non-symmetrical cryptands. Two cryptands (**18** and **20**) were obtained following a modular approach, which implied multiple subsequent steps, starting from the de-symmetrized triazine **3**, while cryptand **27** was synthesized in a two-step procedure similar to the strategy applied for cryptands **21**-**23.**

A comparison between 2,4,6-triaryl-1,3,5-triazine and 1,3,5- triphenyl benzene units as building blocks for molecular cages provided a better overall outcome for the triazine moiety. The use of 2,4,6-triaryl-1,3,5-triazine scaffolds instead of the 1,3,5- triphenyl benzene is more desirable, as the heterocyclic units ensure the planarity of the aromatic central moieties. The hindrance of the *ortho-ortho'* hydrogen atoms of central benzene and of the phenyl groups in 1,3,5-triphenylbenzene determine the torsion of the aromatic substituents resulting in an non-planar structure of the triphenyl benzene unit, while these contacts are missing in 2,4,6-triaryl-1,3,5-triazine, which can therefore adopt a planar structure in an easier manner.

Cryptand **33** was investigated as a building block for accessing higher order molecular architectures, such as cryptand-macrocycle interlocked structures, by exploiting the recently developed active metal template (AMT) approach. In order to conduct this study, three types of azide-alkyne threads (**40**, **44**, **48**) were designed, synthesized and characterized. The results yielded some interesting insights into the active metal template approach towards cryptand-macrocycle architectures, as well as offering new perspectives for investigating cryptand **20** as a key constituent of more intricate mechanically interlocked architectures such as crypto-catenanes.

The complexation ability of cryptands **21-23** for alkali cations and the diprotonated 1,5-naphthalenediamine was investigated by mass spectrometry and NMR studies. The ES(+)-HRMS studies revealed that all investigated cryptands **21-23** displayed the highest complexation preference for the K^+ ion, with a lower affinity of the smallest cryptand **21** towards the main alkali cations, compared to the larger cage molecules **22** and **23**. The ES(+)-MS complexation studies of the larger cage molecule **23** with 1,5-naphthalenediamine revealed the formation of double-charged species corresponding to the complex formed between the cryptand, the mono or diprotonated diamine and/or an alkali cation (Na^+ or K^+). The NMR investigations revealed the formation of a host-guest complex between **23** and the dication of 1,5-naphthylenediamine which resulted in a significant shifting of the aromatic signals in the spectrum of the complex as compared to the spectra of the isolated host and guest molecules.

Keywords:

1,3,5-tris(phenyl)-1,3,5- triazine, 1,3,5-triphenylbenzene, cage molecule, cryptand, active metal template, mechanically interlocked molecules, molecular recognition, complexation, host-guest, macrocycle, non-symmetrical cryptand